Analysis of the ECGI inverse problem solution with respect to the measurement boundary size and the distribution of noise

Mohammed Addouche, Nadra Bouarroudj, Fadhel Jday, Jacques Henry, Nejib Zemzemi

Mathematical Modelling of Natural Phenomena
Math. Model. Nat. Phenom. www.mmnp-journal.org
https://doi.org/10.1051/mmnp/180144

ANALYSIS OF THE ECGI INVERSE PROBLEM SOLUTION WITH RESPECT TO THE MEASUREMENT BOUNDARY SIZE AND THE DISTRIBUTION OF NOISE

Mohammed Addouche[1], Nadra Bouarroudj[2], Fadhel Jday[3], Jacques Henry[4,5] and Nejib Zemzemi[4,5]

Abstract. In this work, we analyze the influence of adding a body surface missing data on the solution of the electrocardiographic imaging inverse problem. The difficulty comes from the fact that the measured Cauchy data is provided only on a part of the body surface and thus a missing data boundary is adjacent to a measured boundary. In order to construct the electrical potential on the heart surface, we use an optimal control approach where the unknown potential at the external boundary is also part of the control variables. We theoretically compare this case to the case where the Dirichlet boundary condition is given on the full accessible surface. We then compare both cases and based on the distribution of noise in the measurements, we conclude whether or not it is worth to use all the data. We use the method of factorization of elliptic boundary value problems combined with the finite element method. We illustrate the theoretical results by some numerical simulations in a cylindrical domain. We numerically study the effect of the size of the missing data zone on the accuracy of the inverse solution.

Mathematics Subject Classification. 12A34, 56B78 .

November 15, 2018.

1. Introduction

Electrocardiographic imaging (ECGI) is a new technology that allows to non-invasively reconstruct the electrical activity of the heart from measurements on the body surface and geometrical information of the torso. This clinical tool is used by cardiologists in order to localize arrhythmogenic substrates, such as atrial and ventricular fibrillations. The current clinical tool consists of a vest containing 252 electrodes that are used to measure the electrical potential at the body surface and software used to calculate the electrical potential on the heart surface. These electrodes are distributed on the body surface. The mathematical method used behind the tool is the Method of Fundamental Solutions (MFS) presented in the work by Wang and Rudy [25]. However, the 252 electrodes are not equally distributed on the torso surface and some regions are more covered than

Keywords. Inverse problem; electrocardiography imaging; Factorization method; Riccati equations.

[1] Abou Bekr Belkaid University, Tlemcen, Algeria. e-mail: `addouchelmd@gmail.com`

[2] Department of Mathematics and informatics, ENP, Oran,Maurice Audin, Algeria. e-mail: `nadra.belaib@yahoo.fr`

[3] Umm al-Qura University, Mekkah KSA. e-mail: `fadheldj@yahoo.com`

[4] INRIA, Bordeaux Sud-Ouest, 200 Avenue de la vielle Tour 33405 Talence Cedex France. e-mail: `Jacques Henry & nejib.zemzemi@inria.fr`

[5] IHU LIRYC, Electrophysiology and Heart Modeling Institute, Pessac, France.

others. Moreover, in clinical practice some electrodes are not considered in the inverse problem. Sometimes because they are not in contact with the patient's skin and sometimes because of the high noise registered on some electrodes. This means that there are regions where we know the potential and others where we don't have any information. But in both cases, we know that we have zero flux boundary condition on the whole body surface. In different studies, for instance John et al. [11], Ghodrati et al. [13] and Oostendorp et al. [23], authors reconstruct these missing BSPs by interpolating them from the well-measured signals: In this case Oostendorp et al. [23] used a Laplacian interpolation of the electrical potential on the body surface. Burnes et al. [11] presented a forward-inverse method, where they solved the inverse problem on an intermediate surface between the torso and the heart surfaces using the recorded potential by the electrodes. Then they solved the forward problem to recover the potential on the whole body surface. Once they have the value of the potential on the whole body surface, they solved the ECGI inverse problem to obtain the potential on the heart surface. Ghodrati et al. [13] used a Bayesian approach to interpolate the electrical PSPs before solving the inverse problem. In a recent work, Bear et al. [8] showed that in some cases the interpolation does not improve the inverse solution and sometimes it even worsens the quality of the reconstructed potentials. In almost of the cited works as well as most of reported in the literature for solving the ECGI inverse problem, the mathematical problem was formulated using a transfer matrix approach. This approach has been first introduced by Roger et al. [7]. The transfer matrix was later computed using different approaches like boundary elements, finite elements or MFS. Recent works (Bouyssier et al. [10]; Hariga et al. [15]; Zemzemi, [26]; Zemzemi et al. [27]) presented novel approaches based on recent advances in boundary-value inverse problem techniques. These works use an energy-based cost function. The theoretical study of these methods has been reported by Ben Abda et al. [1], Andrieux et al. [5] and Azaiez et al. [6]. In this work we use the method of boundary value factorization introduced for solving data completion by Ben Abda et al. [1], which has already been used for solving the ECGI problem in the work by Bouyssier et al. [10]. Our goal in this work is to introduce a new mathematical formulation that takes into account the missing data on the body surface without using interpolation methods. The missing BSPs would be part of the control problem. However, applied to the ECGI inverse problem, the methodology developed in this paper may be applied to any data completion problem for the Laplace equation with missing data on the accessible boundary.

2. Continuous Problem and Factorization Method

For the sake of simplicity we study a model problem where the considered domain is a cylinder. The cylindrical geometry and the Laplace operator make the presentation of the factorization method easier. The method can be generalized to regular non-cylindrical domains and to more general self-adjoint second-order elliptic operators. The generalization for a three dimensional realistic domain can be done and will be presented in a further article.

Let's consider the cylindrical domain Ω is a cylinder in $\mathbb{R}^n$, $\Omega =]0, a[\times \mathcal{O}$, where $\mathcal{O}$ is a bounded domain in $\mathbb{R}^{n-1}$. The length of the cylinder a is a strictly positive real number. We denote by $\partial\Omega$ the boundary of the cylinder: $\partial\Omega = \Gamma_0 \cup \Gamma_a \cup \Sigma$, where $\Sigma =]0, a[\times \partial\mathcal{O}$ is the lateral boundary of Ω, $\Gamma_0 = \Gamma_0^m \cup \Gamma_0^u = \{0\} \times \mathcal{O}$ and $\Gamma_a = \{a\} \times \mathcal{O}$ are the faces. The section $\mathcal{O}$ could be partitioned as $\mathcal{O} = \mathcal{O}^m \cup \mathcal{O}^u$, so that $\{0\} \times \mathcal{O}^m = \Gamma_0^m$ and $\{0\} \times \mathcal{O}^u = \Gamma_0^u$. We suppose that Γ_0 is an accessible boundary, which means that we can construct the electrical potential. On the other hand Γ_a is an inaccessible boundary, which means that we can't construct any measurements on it. For the reasons mentioned previously, the boundary Γ_0^m is the part of Γ_0 where we have measurements of the potentials and in Γ_0^u we don't have electrical potential measurements. We denote by $x \in \mathbb{R}$ the coordinate along the axis of the cylinder and by $y \in \mathbb{R}^{n-1}$ the coordinates in the section, perpendicular to the axis. The schematic representation of the domain Ω and all its boundaries is represented in Figure (1).

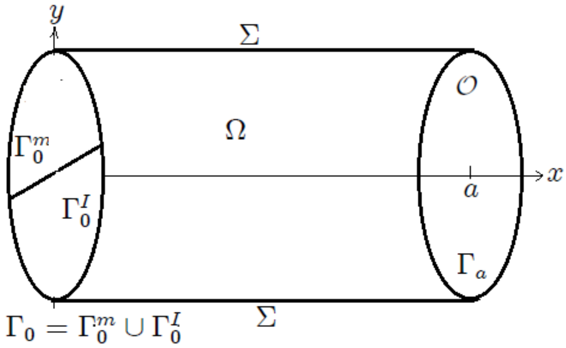

FIGURE 1. Schematic representation of the cylindrical domain used in the study.

2.1. **Statement of the Problem**

In this paper, we consider the following problem on Ω with Cauchy data on Γ_0^m:

$$(\mathcal{P}_0)\begin{cases} -\Delta u = 0 & \text{in} \quad \Omega, \\ u = 0 & \text{on} \quad \Sigma, \\ \dfrac{\partial u}{\partial n} = 0 & \text{on} \quad \Gamma_0, \\ u = T & \text{on} \quad \Gamma_0^m. \end{cases}$$

We recall the Sobolev space $H_{00}^{\frac{1}{2}}(\mathcal{O})$ defined in Theorem 11.7, p.72 of [21] as the $\frac{1}{2}$ interpolate between $H_0^1(\mathcal{O})$ and $L^2(\mathcal{O})$ and we denote by $\left(H_{00}^{\frac{1}{2}}(\mathcal{O})\right)'$ its dual space. The boundary Γ_0^m is the measured portion of the surface of Γ_0 i.e the part of Γ_0 where we have both Dirichlet ($u = T$) and Neumann ($\dfrac{\partial u}{\partial n} = 0$) boundary conditions. The boundary Γ_0^u is the unmeasured part of the surface Γ_0 i.e. it is the part of Γ_0 where we only know that we have a Neumann boundary condition ($\dfrac{\partial u}{\partial n} = 0$), whereas no boundary condition is available on Γ_a. The aim of this paper is to recover these missing boundary data exploiting the over-specified data on Γ_0^m. The existence of a solution of this problem is not insured for arbitrary Cauchy data. This problem is treated in [5], [12], [2] in a general domain Ω having a boundary: $\partial\Omega = \Gamma_0 \cup \Gamma_a$. In [5] the missing boundary data recovery problem is rephrased as a control problem with two states, each one satisfying one boundary condition on Γ_0^m, the control being the unknown boundary conditions on Γ_a. The numerical methods proposed in [3–5] are iterative and therefore, for each new data, they require the resolution of many intermediate forward problem to solve the data completion problem . In the electrocardiography application, one should solve the Cauchy problem at many time steps in order to recover the dynamics of the electrical wave on the heart. For certain pathologies, one should solve the Cauchy problem hundreds or thousands of times in order to obtain the dynamics of the electrical information on the heart surface. In terms of computational cost, this reduces the competitiveness of the iterative methods like in [5], [15], [2], [20] and [26]) and gives more advantage for mesh-free methods like MFS ([25]), where a transfer matrix is computed once for all. In this work we use the same energy function as defined in [5], but we formulate it at the continuous level using Dirichlet-Neumann and Neumann-Dirichlet mappings. These operators are time-independent; they only depend on the geometry. After computing these operators, we compute the inverse solution by solving a linear problem on Γ_a. We make use of the factorization method which transforms the elliptic boundary value problem into two parabolic ones. This approach allows to compute with a good accuracy the Dirichlet-Neumann and Neumann-Dirichlet mappings on a sequence of surfaces flowing from Γ_0 to Γ_a. It allows the direct evaluation of the missing boundary data for any new Cauchy data without re-computation of the operators.

3. Formulation of the data completion problem as an optimal control problem

We assume we know exactly the observation T on Γ_0^m corresponding to the boundary value problem and we seek to determine the Dirichlet and Neumann boundary conditions on Γ_a and Γ_0^u supplementing the problem $(\mathcal{P}_0)$, i.e. the data of the electric potential τ and its derivative η on the surface Γ_a and the potential τ' on Γ_0^u such that the overdetermined boundary value problem $(\mathcal{P}_0)$ given by:

$$\begin{cases} -\Delta u = 0 & \text{in} \quad \Omega, \\ u = 0 & \text{on} \quad \Sigma, \\ \dfrac{\partial u}{\partial n} = 0 & \text{on} \quad \Gamma_0, \\ u = T & \text{on} \quad \Gamma_0^m, \\ u = \tau' & \text{on} \quad \Gamma_0^u, \\ u = \tau, \ \dfrac{\partial u}{\partial n} = \eta & \text{on} \quad \Gamma_a, \end{cases}$$

has a solution. By Holmgren's theorem such conditions are unique and we denote them respectively by t, φ, and $\hat{\tau'}$. In the real life inverse cardiac imaging application, the torso surface Γ_0 has it self no boundary. In the simplified cylindrical case, in order to avoid unnecessary technicalities, we make the following assumption $(\mathcal{H})$ on the subset Γ_0^m and Γ_0^u of Γ_0:

$$(\mathcal{H}) \begin{cases} \text{either } \partial\Gamma_0 \subset \partial\Gamma_0^m \\ \text{or } \partial\Gamma_0 \cap \partial\Gamma_0^m = \varnothing. \end{cases}$$

To deal with well posed problems we have to make precise the spaces where T is given and τ' is sought. For that purpose we need the following lemma.

Lemma 3.1. *Consider the open bounded set $\Omega \subset \mathbb{R}^n$ with regular boundary Γ. Assume Ω is separated into two open parts Ω_0 and Ω_1 with a common boundary γ_0^1: $\Omega = \Omega_0 \cup \gamma_0^1 \cup \Omega_1$, satisfying the assumption $(\mathcal{H})$. Let $u \in H_{00}^{\frac{1}{2}}(\Omega)$ such that $u \equiv 0$ in Ω_1. Then $u\,|_{\Omega_0} \in H_{00}^{\frac{1}{2}}(\Omega_0)$.*

Proof 3.1. *The proof is inspired from that of Theorem 11.7 in [21]. By partition of unity and the use of local maps, the problem is reduced to the simplified geometry: $\Omega = \mathbb{R}^n, \Gamma = \{x_n = 0\}, \Omega_0 = \{x_n < 0\}, \Omega_1 = \{x_n > 0\}$. From Theorem 10.2 p 52 of [21], since $u \in H^{\frac{1}{2}}(\mathbb{R}^n)$, we have :*

$$\left(\int_{\mathbb{R}^n} |u|^2 dx + \sum_{i=1}^{n} \int_0^\infty \mu^{-2} \int_{\mathbb{R}^n} |u(x_1, .., x_i + \mu, ..., x_n) - u(x)|^2 dx d\mu \right)^{\frac{1}{2}} < \infty.$$

Therefore, setting $x = (x', x_n)$, in particular for $i = n$ we have:

$$\left(\int_0^\infty \mu^{-2} \int_{\mathbb{R}^n} |u(x', x_n + \mu) - u(x)|^2 dx d\mu \right)^{\frac{1}{2}} < \infty.$$

But since by assumption $u(x) \equiv 0$ in $x_n < 0$, and as $u \in H^{\frac{1}{2}}(\mathbb{R}^n_+)$, where $R^n_+ = \{x_n > 0\}$, we have:

$$\left(\int_0^\infty \mu^{-2} \int_{\mathbb{R}^n_+} |u(x', x_n + \mu) - u(x)|^2 dx d\mu \right)^{\frac{1}{2}} < \infty.$$

From the two previous estimation, we deduce

$$\left(\int_0^{\infty}\mu^{-2}d\mu\int_{\mathbb{R}^{n-1}}dx'\int_0^{\mu}|u(x',x_n)|^2dxd\mu\right)^{\frac{1}{2}}<\infty.$$

Integrating by parts in t *we have:*

$$\left(\int_{\mathbb{R}^n_+}\frac{1}{x_n}|u(x)|^2dx\right)^{\frac{1}{2}}<\infty.$$

This is the regularity condition in the neighbourhood of Γ *for* u *to belong to* $H^{\frac{1}{2}}_{00}(\Omega_1)$ *(Theorem 11.7 p 66 in [21]).*

Thanks to assumption $(\mathcal{H})$, it is possible to construct a extension $\widetilde{T}$ of T in Γ_0^u such that:

$$T_0=\begin{cases} T \text{ on } \Gamma_0^m \\ \widetilde{T} \text{ on } \Gamma_0^u\end{cases}\quad T_0\in H^{\frac{1}{2}}_{00}\left(\Gamma_0\right).$$

Let γ_m^u be the common boundary to Γ_0^m and Γ_0^u. By $(\mathcal{H})$, γ_m^u is included in an open subset relatively compact in Γ_0. Then the extension can be made locally by symmetry with respect to γ_m^u (cf [21]). The functions $\widetilde{T}$ and τ' have to satisfy some compatibility conditions with T on γ_m^u in order to satisfy the restrictions on Γ_0^u of functions of $H^{\frac{1}{2}}_{00}\left(\Gamma_0\right)$ To avoid this problem we add a bias to τ': instead we will consider as unknown $\tau_0'=\tau'-\widetilde{T}$ on Γ_0^u. Now thanks to lemma 3.1, τ_0' is sought in $H^{\frac{1}{2}}_{00}\left(\Gamma_0^u\right)$.

The data completion problem $(\mathcal{P}_0)$ is converted to an optimal control problem following the approach used in [5], [1] and [10]. The difference is that now it includes three states instead of two. Each of them represents a boundary condition either on the inaccessible boundary Γ_a or on the accessible but unobserved boundary Γ_0^u. For every triplet $(\eta,\tau,\tau_0')\in\left(H^{\frac{1}{2}}_{00}\left(\Gamma_a\right)\right)'\times H^{\frac{1}{2}}_{00}\left(\Gamma_a\right)\times H^{\frac{1}{2}}_{00}\left(\Gamma_0^u\right)$, we define the triplet of states (u_1,u_2,u_3) as follows:

$$(\mathcal{P}_1)\begin{cases}-\Delta u_1=0 & \text{in} & \Omega,\\ u_1=0 & \text{on} & \Sigma,\\ u_1=T & \text{on} & \Gamma_0^m,\\ u_1=\widetilde{T} & \text{on} & \Gamma_0^u,\\ \dfrac{\partial u_1}{\partial n}=\eta & \text{on} & \Gamma_a,\end{cases}\quad,\quad(\mathcal{P}_2)\begin{cases}-\Delta u_2=0 & \text{in} & \Omega,\\ u_2=0 & \text{on} & \Sigma,\\ \dfrac{\partial u_2}{\partial n}=0 & \text{on} & \Gamma_0,\\ u_2=\tau & \text{on} & \Gamma_a,\end{cases}$$

and

$$(\mathcal{P}_3)\begin{cases}-\Delta u_3=0 & \text{in} & \Omega,\\ u_3=0 & \text{on} & \Sigma,\\ u_3=0 & \text{on} & \Gamma_0^m,\\ u_3=\tau_0'=\tau'-\widetilde{T} & \text{on} & \Gamma_0^u,\\ \dfrac{\partial u_3}{\partial n}=0 & \text{on} & \Gamma_a,\end{cases}$$

where η, τ and τ_0' are the control variables. The three states are well defined in $H^1(\Omega)$.
We define the following cost functional depending on the control variables:

$$J(\eta,\tau,\tau_0')=\int_{\Omega}|(\nabla u_1+\nabla u_3)-\nabla u_2|^2dxdy. \tag{3.1}$$

We minimize this functional with respect to η, τ and τ_0' in $\left(H_{00}^{\frac{1}{2}}(\Gamma_a)\right)' \times H_{00}^{\frac{1}{2}}(\Gamma_a) \times H_{00}^{\frac{1}{2}}(\Gamma_0^u)$. Owing to the assumption of perfect observation on Γ_0^m we made, we have that the minimum of J is 0:

$$\inf_{(\eta,\tau,\tau_0')\in\left(H_{00}^{\frac{1}{2}}(\Gamma_a)\right)'\times H_{00}^{\frac{1}{2}}(\Gamma_a)\times H_{00}^{\frac{1}{2}}(\Gamma_0^u)} J(\eta,\tau,\tau_0') = J(\varphi,t,\hat{\tau'}-\widetilde{T}) = 0.$$

Clearly, at the minimum, $u_1(\varphi)+u_3(\hat{\tau'}-\widetilde{T}) = u_2(t)$. We denote Δ_Γ the $(n-1)D$-laplacian on any section Γ_x. The spaces $\left(H_{00}^{\frac{1}{2}}(\Gamma_a)\right)'$ and $H_{00}^{\frac{1}{2}}(\Gamma_a)$ are equipped, respectively, with the following inner product (see [21]):

$$\langle u,v\rangle_{\left(H_{00}^{\frac{1}{2}}(\Gamma_a)\right)'} = \int_{\Gamma_a} (-\Delta_\Gamma)^{-\frac{1}{4}} u (-\Delta_\Gamma)^{-\frac{1}{4}} v dy = \int_{\Gamma_a} u(-\Delta_\Gamma)^{-\frac{1}{2}} v dy,$$

for all u, $v \in \left(H_{00}^{\frac{1}{2}}(\Gamma_a)\right)'$, and

$$\langle u,v\rangle_{H_{00}^{\frac{1}{2}}(\Gamma_a)} = \int_{\Gamma_a} (-\Delta_\Gamma)^{\frac{1}{4}} u (-\Delta_\Gamma)^{\frac{1}{4}} v dy = \int_{\Gamma_a} u(-\Delta_\Gamma)^{\frac{1}{2}} v dy,$$

for all u, $v \in H_{00}^{\frac{1}{2}}(\Gamma_a)$. Similarly

$$\langle u,v\rangle_{H_{00}^{\frac{1}{2}}(\Gamma_0^u)} = \int_{\Gamma_0^u} (-\Delta_\Gamma)^{\frac{1}{4}} u (-\Delta_\Gamma)^{\frac{1}{4}} v dy = \int_{\Gamma_0^u} u(-\Delta_\Gamma)^{\frac{1}{2}} v dy,$$

for all u, $v \in H_{00}^{\frac{1}{2}}(\Gamma_0^u)$. Due to the ill-posedness of the inverse problem, and in particular because of the non-continuity of solutions with respect to the Cauchy data [14] the resolution with noisy observations requires the use of a regularization. We use a Tikhonov regularization and denote by J_ϵ the new cost function:

$$J_\epsilon(\eta,\tau,\tau_0') = J(\eta,\tau,\tau_0') + \epsilon\left(\|\eta\|^2_{\left(H_{00}^{\frac{1}{2}}(\Gamma_a)\right)'} + \|\tau\|^2_{H_{00}^{\frac{1}{2}}(\Gamma_a)} + \|\tau_0'\|^2_{H_{00}^{\frac{1}{2}}(\Gamma_0^u)}\right). \tag{3.2}$$

where ϵ is a non negative regularization parameter. One could use a different parameter for each of the regularization terms. Here, we use the same parameter ϵ just for the sake of simplicity.

4. Brief sketch of the factorization method for boundary value problems

In this section, we show how to apply the factorization method to the states u_1, u_2 and u_3. In the next section we will show we can express the cost function explicitly in terms of the controls η,τ and τ_0' using the operators derived in this section for the factorization. The technique of invariant embedding appeared in the field of the theory of optimal control with Bellman, [9]. The method developed in [16–18] allows to use the factorization approach to solve elliptic boundary value problems. This method is also used in [19] and [1] for solving a data completion problem in a cylindrical domain. Recently this method has been used to solve the inverse problem in electrocardiography for realistic heart and torso geometry [10]. We embed the boundary value problem for the state equation in a family of similar problems defined on Ω_s sub-domains of Ω. For that we define $\Gamma_s = \{s\} \times \mathcal{O}$ a mobile boundary which will move from $s = 0$ to $s = a$. At each position s, one can thus define a sub-domain $\Omega_s =]0, s[\times\mathcal{O}$ with lateral boundary Σ_s delimited by surfaces Γ_0 and Γ_s. The schematic representation of Ω_s is given in Figure 2. The general formulation for non cylindrical geometries could be found in [18].

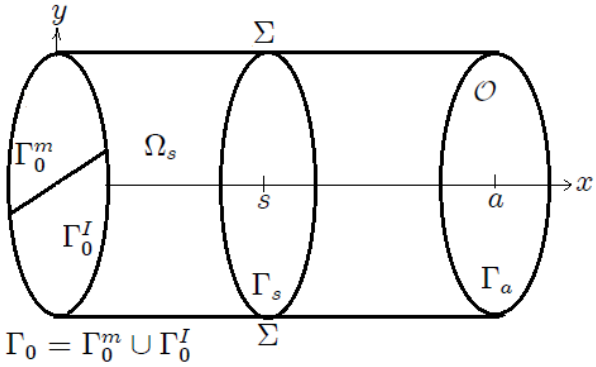

FIGURE 2. Schematic representation of the moving domain Ω_s.

For given boundary data $(\alpha_1, \beta, \alpha_2) \in \left(H_{00}^{\frac{1}{2}}(\Gamma_s)\right)' \times H_{00}^{\frac{1}{2}}(\Gamma_s) \times H_{00}^{\frac{1}{2}}(\Gamma_0^u)$, we define u_1^s, u_2^s and u_3^s solution of the following three problems in Ω_s:

$$(\mathcal{P}_1^s)\begin{cases} -\Delta u_1^s = 0 & \text{in} \quad \Omega_s, \\ u_1^s = 0 & \text{on} \quad \Sigma_s, \\ u_1^s = T & \text{on} \quad \Gamma_0^m, \\ u_1^s = \widetilde{T} & \text{on} \quad \Gamma_0^u, \\ \dfrac{\partial u_1^s}{\partial n} = \alpha_1 & \text{on} \quad \Gamma_s, \end{cases} \qquad (\mathcal{P}_2^s)\begin{cases} -\Delta u_2^s = 0 & \text{in} \quad \Omega_s, \\ u_2^s = 0 & \text{on} \quad \Sigma_s, \\ \dfrac{\partial u_2^s}{\partial n} = 0 & \text{on} \quad \Gamma_0, \\ u_2^s = \beta & \text{on} \quad \Gamma_s, \end{cases}$$

and

$$(\mathcal{P}_3^s)\begin{cases} -\Delta u_3^s = 0 & \text{in} \quad \Omega_s, \\ u_3^s = 0 & \text{on} \quad \Sigma_s, \\ u_3^s = 0 & \text{on} \quad \Gamma_0^m, \\ u_3^s = \alpha_2 & \text{on} \quad \Gamma_0^u, \\ \dfrac{\partial u_3^s}{\partial n} = 0 & \text{on} \quad \Gamma_s, \end{cases}$$

where n is the outward normal to Ω_s.

4.1. **Neumann-Dirichlet mapping**

By splitting problem $(\mathcal{P}_1^s)$ into two well posed problems, we can write u_1^s as a sum of two functions γ_s and δ_s depending linearly on α_1 and T respectively. The functions γ_s and δ_s are solutions of the following two problems:

$$\begin{cases} -\Delta \gamma_s = 0 & \text{in} \quad \Omega_s, \\ \gamma_s = 0 & \text{on} \quad \Sigma_s, \\ \gamma_s = 0 & \text{on} \quad \Gamma_0^m, \\ \gamma_s = 0 & \text{on} \quad \Gamma_0^u, \\ \dfrac{\partial \gamma_s}{\partial n} = \alpha_1 & \text{on} \quad \Gamma_s, \end{cases} \quad \text{and} \quad \begin{cases} -\Delta \delta_s = 0 & \text{in} \quad \Omega_s, \\ \delta_s = 0 & \text{on} \quad \Sigma_s, \\ \delta_s = T & \text{on} \quad \Gamma_0^m, \\ \delta_s = \widetilde{T} & \text{on} \quad \Gamma_0^u, \\ \dfrac{\partial \delta_s}{\partial n} = 0 & \text{on} \quad \Gamma_s. \end{cases}$$

For every $s \in]0, a]$ we define the Neumann-Dirichlet mapping $Q(s)$ by:

$$Q\left(s\right)\alpha_1 = \gamma_s\mid_{\Gamma_s}.$$

We also define the residual part $\omega\left(s\right)$ associated to the operator Q by $\omega\left(s\right) = \delta_s\mid_{\Gamma_s} \in H^{\frac{1}{2}}_{00}\left(\Gamma_s\right)$. We have:

$$u_1^s\mid_{\Gamma_s} = Q\left(s\right)\alpha_1 + \omega\left(s\right).$$

For every s in $]0, a]$, $Q\left(s\right) : \left(H^{\frac{1}{2}}_{00}\left(\Gamma_s\right)\right)' \mapsto H^{\frac{1}{2}}_{00}\left(\Gamma_s\right)$ is a coercive, self-adjoint, linear continuous operator. For $x < s$ that the restriction of $u_1^s(\alpha_1)$ on Ω_x, is a solution of the problem $(\mathcal{P}_1^x)$. By the same calculation as previously we have the relation:

$$u_1^s\left(x, \alpha_1\right) = Q(x)\frac{\partial u_1^s}{\partial x}\left(x, \alpha_1\right) + \omega\left(x\right) \quad . \tag{4.3}$$

For the sake of clarity, from now on, we denote by u_1 (respectively, Q and ω), the restriction on Γ_x $u_1(x)$ (respectively, $Q(x)$ and $\omega(x)$):

$$u_1 = Q\frac{\partial u_1}{\partial x} + \omega. \tag{4.4}$$

In a formal way, we take the derivative of (4.4) with respect to x:

$$\frac{du_1}{dx} = \frac{dQ}{dx}\frac{du_1}{dx} + Q\frac{d^2u_1}{dx^2} + \frac{d\omega}{dx}.$$

By replacing the term $\frac{d^2u_1}{dx^2}$ by $-\Delta_\Gamma u_1$ and substituting u_1, using (4.4) and the fact that α_1 is arbitrary we get:

$$\begin{cases} \dfrac{dQ}{dx} - Q\Delta_\Gamma Q &= I, \\ \dfrac{d\omega}{dx} - Q\Delta_\Gamma \omega &= 0. \end{cases}$$

One can extend by continuity this argument to $x = 0$. Writing relation (4.3) at $x = 0$, and by using the fact that $u_1(0)$ is arbitrary, we get the initial conditions $Q\mid_{\Gamma_0} = 0$, $\omega\mid_{\Gamma_0^m} = T$ and $\omega\mid_{\Gamma_0^u} = \tilde{T}$. Adding the condition on Γ_a for u_1, we summarize the result in an equivalent formulation of $(\mathcal{P}_1)$:

$$\begin{cases} \dfrac{dQ}{dx} - Q\Delta_\Gamma Q = I & Q_{|\Gamma_0} = 0, \\ \dfrac{d\omega}{dx} - Q\Delta_\Gamma \omega = 0 & \omega\mid_{\Gamma_0^m} = T, \quad \omega\mid_{\Gamma_0^u} = \tilde{T}, \\ u_1 = Q\dfrac{\partial u_1}{\partial x} + \omega & \dfrac{\partial u_1}{\partial x}\mid_{\Gamma_a} = \eta. \end{cases} \tag{4.5}$$

4.2. **Dirichlet-Neumann mapping**

We use the same methodology as in the previous paragraph. We define the Dirichlet-Neumann mapping $P(s)$ as the linear operator that maps β to $\frac{\partial u_2^s}{\partial x}\mid_{\Gamma_s}$. Again, for all $x < s$ the restriction $u_2^s\left(x\right)$ satisfies:

$$\frac{\partial u_2^s}{\partial x}\left(x\right) = P\left(x\right)u_2^s\left(x\right),$$

or simply:

$$\frac{\partial u_2^s}{\partial x} = Pu_2^s. \tag{4.6}$$

Taking the derivative with respect to x:

$$\frac{d^2u_2^s}{dx^2} = \frac{dP}{dx}u_2^s + P\frac{\partial u_2^s}{\partial x},$$

and substituting u_2^s, using $(\mathcal{P}_2^s)$, taking $x = s$ and using the fact that β is arbitrary we deduce:

$$\frac{dP}{dx} + P^2 = -\Delta_\Gamma.$$

We can extend by continuity this argument to $x = 0$. Using the fact that $u_2(0)$ is arbitrary and that the flux of u_2 over Γ_0 is equal to zero, we get the initial conditions for P, $\quad P\mid_{\Gamma_0}= 0$. Adding the condition on Γ_a for u_2, we summarize the result: an equivalent formulation of $(\mathcal{P}_2)$ is:

$$\left\{\begin{array}{ll} \dfrac{dP}{dx} + P^2 = -\Delta_\Gamma & \quad P\mid_{\Gamma_0}= 0, \\ \dfrac{\partial u_2}{\partial x} = Pu_2 & \quad u_2\mid_{\Gamma_a}= \tau. \end{array}\right. \tag{4.7}$$

4.3. **New operators related to the incomplete measurement**

We consider the family of problems $(\mathcal{P}_3^s)$. For every s in $]0, a]$ we define a new Dirichlet-Neumann mapping S as the linear operator that maps α_2 to $\frac{\partial u_3^s}{\partial x}\mid_{\Gamma_0^u}$. We note that the operator S is well defined, because for any α_2 we can solve problem $(\mathcal{P}_3^s)$. Then by linearity of the problem $(\mathcal{P}_3^s)$, so by the well-posedness of the problem on u_3^s and the continuity of the trace mapping we define, for every s in $]0, a]$, the operator $S\,(s)$ as follows:

$$\begin{array}{rl} S\,(s): & H_{00}^{\frac{1}{2}}\left(\Gamma_0^u\right) \mapsto \left(H_{00}^{\frac{1}{2}}\left(\Gamma_0^u\right)\right)' \\ & \alpha_2 \mapsto \dfrac{\partial u_3^s}{\partial s}\left(\alpha_2\right)\mid_{\Gamma_0^u}= S\,(s)\,\alpha_2. \end{array}$$

$S\,(s)$ is a coercive, self-adjoint, linear continuous operator. For further calculations, we simplify the notation by writing:

$$\frac{\partial u_3^s}{\partial s} = Su_3^s. \tag{4.8}$$

By defining the extension operator R and projection operators Π_u and Π_m:

$$\begin{array}{rl} R: & H_{00}^{\frac{1}{2}}\left(\Gamma_0^u\right) \mapsto H_{00}^{\frac{1}{2}}\left(\Gamma_0\right) \\ & \alpha_2 \mapsto \alpha_2^0 = \left\{\begin{array}{l} \alpha_2 \text{ in } \Gamma_0^u, \\ 0 \text{ in } \Gamma_0^m, \end{array}\right. \end{array}$$

$$\begin{array}{rl} \Pi_u: & \left(H_{00}^{\frac{1}{2}}\left(\Gamma_0\right)\right)' \mapsto \left(H^{\frac{1}{2}}\left(\Gamma_0^u\right) \cap H_{00}^{\frac{1}{2}}\left(\Gamma_0\right)\right)' \\ & g \mapsto g\mid_{\Gamma_0^u}, \\ \Pi_m: & \left(H_{00}^{\frac{1}{2}}\left(\Gamma_0\right)\right)' \mapsto \left(H^{\frac{1}{2}}\left(\Gamma_0^m\right) \cap H_{00}^{\frac{1}{2}}\left(\Gamma_0\right)\right)' \\ & g \mapsto g\mid_{\Gamma_0^m}, \end{array}$$

and using the symmetry transformation $x \to a - x$ of the cylindrical domain Ω, we obtain the following relation between the Dirichlet-Neumann operators S and P:

$$S(s) = \Pi_u \circ P(s) \circ R,$$

where $\circ$ is the composition sign.
We also define for every s in $]0,a]$ the operator H as follows:

$$\begin{aligned} H(s): \quad & H_{00}^{\frac{1}{2}}(\Gamma_0^u) \mapsto H_{00}^{\frac{1}{2}}(\Gamma_s) \\ & \alpha_2 \mapsto u_3^s(\alpha_2)\,|_{\Gamma_s} = H(s)\,\alpha_2. \end{aligned}$$

The linear operator H could be constructed based on the residual ω defined in (4.1). In fact, for a given $\alpha_2 \in H_{00}^{\frac{1}{2}}(\Gamma_0^u)$, $H(s)\alpha_2$ corresponds to the residual ω with the initial condition $\omega(0) = R\alpha_2$.
The new operator P' is defined as follows:

$$\begin{aligned} P'(s): \quad & H_{00}^{\frac{1}{2}}(\Gamma_0) \mapsto \left(H_{00}^{\frac{1}{2}}(\Gamma_0)\right)' \\ & T_0 \mapsto \frac{\partial u_1'}{\partial s}\,|_{\Gamma_0} = P'(s)\,T_0, \end{aligned} \tag{4.9}$$

where $T_0 = \begin{cases} T \text{ on } \Gamma_0^m \\ \tilde{T} \text{ on } \Gamma_0^u \end{cases}$, and u_1' is the solution of:

$$\begin{cases} -\Delta u_1' = 0 & \text{in} \quad \Omega_s, \\ u_1' = 0 & \text{on} \quad \Sigma_s, \\ \dfrac{\partial u_1'}{\partial n} = 0 & \text{on} \quad \Gamma_s, \\ u_1' = T_0 & \text{on} \quad \Gamma_0. \end{cases}$$

This operator satisfies:

$$\frac{dP'}{ds}(s) + (P')^2(s) = -\Delta_\Gamma \qquad P'(0) = 0.$$

By the uniqueness of the solution of the Riccati equation and due the symmetry of the cylindrical domain, P' is identical to P but we keep the notation P' to recall that we use it on Γ_0.

5. Solving the optimal control problem

The method of invariant embedding used in the factorization of the state equations is of the same nature as the one used to factorize optimal control problems. Indeed, the energy functional J can be expressed directly in terms of the control variables η, τ and τ' using the operators P, Q, S and H. So there is no need to introduce an adjoint state to derive the optimality condition. Saying it in another way, the classical decoupling of the optimality system between state and adjoint state using a Riccati equation is performed here at the same time as the factorization of the state equation.
From now we will denote $P = P(a)$, $Q = Q(a)$, $S = S(a)$ and $H = H(a)$. Let A be the matrix operator defined as follows

$$A = \begin{pmatrix} Q & -QP & 0 \\ -PQ & P & -PH \\ 0 & -H^*P & S \end{pmatrix}, \tag{5.10}$$

H^* is the adjoint operator of H. Let us denote $[\eta,\tau,\tau_0']$ the row vector with components η,τ and τ_0'. Let us remark that in relation to the ill-posedness of the Cauchy problem, the operator A is not coercive, but it is self-adjoint.

Proposition 5.1. *The cost functional J can be written equivalently,*

$$J(\eta,\tau,\tau_0') \quad = \quad K \quad + \quad (\eta,\tau,\tau_0')\, A \begin{pmatrix} \eta \\ \tau \\ \tau_0' \end{pmatrix} \quad - \quad 2\,\langle \omega(T_0), P\tau\rangle_{\Gamma_a} \quad + \quad 2\,\langle \tau_0', \Pi_u \circ P' T_0\rangle_{\Gamma_0^u}, \quad (5.11)$$

where K is a constant that does not depend on η,τ and τ_0'. If a minimum of J is reached at the triplet (φ,t,t'), it satisfies:

$$A\,[\varphi,t,t']\,' = [0, P\omega(T_0), -\Pi_u \circ P\,'T_0]' \,. \quad (5.12)$$

Proof 5.1. *Let λ_1, λ_2 be the solutions of:*

$$\begin{cases} -\Delta\lambda_1 = 0 & in \quad \Omega, \\ \lambda_1 = T_0 & on \quad \Gamma_0, \\ \dfrac{\partial\lambda_1}{\partial n} = 0 & on \quad \Gamma_a. \end{cases}, \qquad \begin{cases} -\Delta\lambda_2 = 0 & in \quad \Omega, \\ \lambda_2 = \tau_0' & on \quad \Gamma_0, \\ \dfrac{\partial\lambda_2}{\partial n} = 0 & on \quad \Gamma_a. \end{cases}$$

and $\lambda = \lambda_1 + \lambda_2$ satisfies

$$\begin{cases} -\Delta\lambda = 0 & in \quad \Omega, \\ \lambda = T' & on \quad \Gamma_0, \\ \dfrac{\partial\lambda}{\partial n} = 0 & on \quad \Gamma_a. \end{cases}$$

where $T' = \begin{cases} T \;\; on \;\; \Gamma_0^m, \\ \tau' \;\; on \;\; \Gamma_0^u. \end{cases}$

To alleviate notations, we will abusively denote duality pairings with integrals. We set $v_1 = u_1 + u_3$, applying Green's formula to cost functional (3.1) then:

$$\begin{aligned} J(\eta,\tau,\tau_0') &= \int_\Omega |\nabla v_1 - \nabla u_2|^2\, dxdy \\ &= \int_{\Gamma_0} \frac{\partial v_1}{\partial n}(T' - u_2)dy + \int_{\Gamma a} \left(\eta - \frac{\partial u_2}{\partial n}\right)(v_1 - \tau)\, dy \end{aligned}$$

Using the full Green's formula for the term in $\dfrac{\partial v_1}{\partial n} u_2$

$$J(\eta,\tau,\tau_0') = \int_{\Gamma_0} \frac{\partial v_1}{\partial n}\lambda dy + \int_{\Gamma_a} \left(\eta\tau - v_1 \frac{\partial u_2}{\partial n}\right) dy + \int_{\Gamma a} \left(\eta - \frac{\partial u_2}{\partial n}\right)(v_1 - \tau)\, dy$$

and for the terms in $\dfrac{\partial v_1}{\partial n}$

$$J(\eta,\tau,\tau_0') = \int\limits_{\Gamma_0} T'\nabla\lambda\cdot n dy + \int\limits_{\Gamma_a} \left(\eta\,(v_1-\lambda) + \frac{\partial u_2}{\partial n}\tau\right) dy - 2\int\limits_{\Gamma a} v_1 \frac{\partial u_2}{\partial n} dy. \tag{5.13}$$

From (4.4), (4.6) and from the definition of λ $(\lambda(a)=\omega(a))$ *we obtain*

$$J(\eta,\tau,\tau_0') = \int\limits_{\Gamma_0} T'\frac{\partial\lambda}{\partial n} dy + \int\limits_{\Gamma_a} (\eta Q\eta + \tau P\tau)\, dy - 2\int\limits_{\Gamma a} (Q\eta + \omega(T'))\, P\tau dy \tag{5.14}$$

From the definition of T' *and* λ *we have:*

$$\int\limits_{\Gamma_0} T'\frac{\partial\lambda}{\partial n} dy = \int\limits_{\Gamma_0^m} T\frac{\partial\lambda_1}{\partial n}\, d\Gamma_0^m + \int\limits_{\Gamma_0^u} \tau'\frac{\partial\lambda_1}{\partial n}\, d\Gamma_0^u + \int\limits_{\Gamma_0^m} T\frac{\partial\lambda_2}{\partial n}\, d\Gamma_0^m + \int\limits_{\Gamma_0^u} \tau'\frac{\partial\lambda_2}{\partial n}\, d\Gamma_0^u \tag{5.15}$$

where the term $K := \int\limits_{\Gamma_0^m} T\frac{\partial\lambda_1}{\partial n}\, d\Gamma_0^m$ *does not depend on controls* η,τ *and* τ_0'. *According to the definition of operators* S, P', Π_m *and* Π_u, *we have*

$$\frac{\partial\lambda_2}{\partial n}\,|_{\Gamma_0^u} = S\tau_0', \quad \frac{\partial\lambda_1}{\partial n}\,|_{\Gamma_0^u} = \Pi_u\circ P'T_0, \quad \frac{\partial\lambda_2}{\partial n}\,|_{\Gamma_0^m} = \Pi_m\circ P'\tau_0', \tag{5.16}$$

We denote $\omega(T')$ *by* $\omega(T;\tau')$ *in order to show the dependency of* ω *on the data on* Γ_0^m *and* Γ_0^u. *We have:*

$$\omega(T') = \omega(T;\tau') + \omega(0;\tau_0') = \omega(T_0) + H\tau_0' \tag{5.17}$$

Substituting (5.15), (5.16) and (5.17) in (5.14) we obtain

$$\begin{aligned} J(\eta,\tau,\tau_0') \;=\;& K + \int\limits_{\Gamma_0^u} \tau'\Pi_u\circ P'T_0\, d\Gamma_0^u + \int\limits_{\Gamma_0^m} T\Pi_m\circ P'\tau_0'\, d\Gamma_0^m + \int\limits_{\Gamma_0^u} \tau' S\tau_0'\, d\Gamma_0^u \\ &+ \int\limits_{\Gamma_a} (\eta Q\eta + \tau P\tau)\, d\Gamma_a - 2\int\limits_{\Gamma_a} (Q\eta + \omega(T_0))\, P\tau\, d\Gamma_a \\ &-2\int\limits_{\Gamma_a} H\tau_0' P\tau\, d\Gamma_a. \end{aligned} \tag{5.18}$$

The third right-hand side term could be developed as follows

$$\begin{aligned}\int_{\Gamma_0^m} T\Pi_m \circ P'\tau_0'\, d\Gamma_0^m &= \int_{\Gamma_0^m} u_1' \frac{\partial \lambda_2}{\partial n}\, d\Gamma_0^m \\ &= -\int_{\Gamma_0^u} u_1' \frac{\partial \lambda_2}{\partial n}\, d\Gamma_0^u + \int_{\Omega} \nabla u_1' \nabla \lambda_2 d\Omega \\ &= -\int_{\Gamma_0^u} \tilde{T} S\tau_0'\, d\Gamma_0^u + \int_{\Gamma_0^u} \frac{\partial u_1'}{\partial n} \lambda_2\, d\Gamma_0^u \\ &= -\int_{\Gamma_0^u} \tilde{T} S\tau_0'\, d\Gamma_0^u + \int_{\Gamma_0^u} \tau_0' \Pi_u \circ P' T_0\, d\Gamma_0^u \end{aligned} \tag{5.19}$$

By substituting (5.19) in (5.18), we obtain

$$\begin{aligned} J(\eta,\tau,\tau_0') &= K' + \int_{\Gamma_0^u} \tau_0'\Pi_u \circ P'T_0\, d\Gamma_0^u + \int_{\Gamma_0^u} \tau_0'\Pi_u \circ P'T_0\, d\Gamma_0^u + \int_{\Gamma_0^u} \tau_0' S\tau_0'\, d\Gamma_0^u + \\ & \int_{\Gamma_a} (\eta Q\eta + \tau P\tau)\; d\Gamma_a - 2\int_{\Gamma_a} (Q\eta + \omega(T_0))\, P\tau\, d\Gamma_a - 2\int_{\Gamma_0^u} \tau_0' H^* P\tau\, d\Gamma_0^u, \end{aligned}$$

where we set $K' = K - \int_{\Gamma_0^u} \widetilde{T}\Pi_u \circ P'T_0\, d\Gamma_0^u$. *This formula can be written as (5.11) taking into account that* P, Q, S *are self-adjoint.*

Deriving the functional J *with respect to* η, τ *and* τ_0', *we obtain*

$$\begin{aligned} \langle \frac{\partial J}{\partial \eta}, \psi\rangle &= 2\int_{\Gamma_a} Q\eta\psi\, d\Gamma_a - 2\int_{\Gamma_a} QP\tau, \psi\, d\Gamma_a, \\ \langle \frac{\partial J}{\partial \tau}, \varphi\rangle &= 2\int_{\Gamma_a} P\tau\varphi\, d\Gamma_a - 2\int_{\Gamma_a} PQ\eta\varphi\, d\Gamma_a - 2\int_{\Gamma_a} PH\tau_0'\varphi\, d\Gamma_a - 2\int_{\Gamma_a} P\omega(T_0)\varphi\, d\Gamma_a, \\ \langle \frac{\partial J}{\partial \tau_0'}, \mu\rangle &= 2\int_{\Gamma_0^u} \Pi_u \circ P'T_0\mu\, d\Gamma_0^u + 2\int_{\Gamma_0^u} S\tau_0'\mu\, d\Gamma_0^u - 2\int_{\Gamma_0^u} H^* P\tau\mu\, d\Gamma_0^u. \end{aligned}$$

Thus, when the observation on Γ_0^m *is exact, the optimum of* J *is reached at* (φ, t, t_0') *satisfying the following linear system*

$$Q\varphi - QPt = 0, \tag{5.20}$$
$$-PQ\varphi + Pt - PH\, t_0' = P\omega(T_0), \tag{5.21}$$
$$-H^* Pt + S\, t_0' = -\Pi_u \circ P'T_0. \tag{5.22}$$

6. Comparison between cases of complete and incomplete observations

In this section, we will analyse the effect of regularization and noise on the solution of the data completion problem both when considering complete and incomplete observation on the accessible boundary.

6.1. **Incomplete observation**

In this paragraph, we present an analysis of the Tikhonov regularization in the cylindrical case where the observation of the electrical potential is performed on a part of the accessible boundary $\Gamma_0^m \subset \Gamma_0$ as previously presented. The goal is to estimate how the error between the exact and the regularized problem solution behaves with respect to the size of Γ_0^m and the introduced noise ($u = T + \delta$). We follow the approach developed by Morozov and Stessin [22]. We recall that the cost function with the Tikhonov regularization term defined in (3.2) is

$$J_\epsilon(\eta, \tau, \tau_0') = J(\eta, \tau, \tau_0') + \epsilon \left(\|\eta\|^2_{\left(H^{\frac{1}{2}}_{00}(\Gamma_a)\right)'} + \|\tau\|^2_{H^{\frac{1}{2}}_{00}(\Gamma_a)} + \|\tau_0'\|^2_{H^{\frac{1}{2}}_{00}(\Gamma_0^u)} \right)$$

Thus, from Proposition 5.1, the optimum of J_ϵ is reached at $(\varphi_\epsilon, t_\epsilon, t_\epsilon')$ satisfying the following linear system

$$\begin{aligned} (\epsilon I + Q)\,\varphi_\epsilon - QPt_\epsilon &= 0, && (6.23)\\ -PQ\varphi_\epsilon + (\epsilon I + P)\,t_\epsilon - PH\,t_\epsilon' &= P\omega(T_0), && (6.24)\\ -H^*Pt_\epsilon + (\epsilon I + S)\,t_\epsilon' &= -\Pi_u \circ P'T_0. && (6.25) \end{aligned}$$

Denoting by $A_\epsilon = A + \epsilon I$, we have

$$A_\epsilon\,[\varphi_\epsilon, t_\epsilon, t'_\epsilon]' = [0, P\omega(T_0), -\Pi_u \circ P\,'T_0]'\,. \qquad (6.26)$$

Adding a noise $\delta \in L^2(\Gamma_0^m)$ to the exact observable data T, we denote by $(\varphi_\epsilon^\delta, t_\epsilon^\delta, {t'}_\epsilon^\delta)$, the solution of the regularized problem but with noisy observation $T + \delta$. Obviously, this triplet satisfies

$$A_\epsilon \left[\varphi_\epsilon^\delta, t_\epsilon^\delta, {t'}_\epsilon^\delta\right]' = [0, P\omega(T_0 + \delta), -\Pi_u \circ P\,'\,(T_0 + \delta)]'\,. \qquad (6.27)$$

In what follows our aim is twofold. First, we would like to estimate the error between t_ϵ^δ and the exact solution t at the inaccessible boundary Γ_a. Second we want to quantify the effect of the size of Γ_0^m on the error $\| t_\epsilon^\delta - t \|_{L^2(\Gamma_a)}$.

Following the Morozov's approach, we first apply a Cholesky factorization to the operator A.

$$A = R^*R \quad \text{where } R = \begin{pmatrix} B & C & 0 \\ 0 & D & E \\ 0 & 0 & F \end{pmatrix}.$$

By identification, we have

$$\begin{cases} B = Q^{\frac{1}{2}}, \\ C = -Q^{\frac{1}{2}}P, \\ D = (P - PQP)^{\frac{1}{2}}, \\ E = -(P - PQP)^{-\frac{1}{2}}PH, \\ F = \left[S - H^*P(P - PQP)^{-1}PH\right]^{\frac{1}{2}}. \end{cases}$$

Theorem 6.1. *There exist a decaying positive sequence* $(h_\epsilon)_{\epsilon>0}$

$$h_\epsilon \longrightarrow 0 \text{ for } \epsilon \longrightarrow 0,$$

a non negative constant k_1 that depends only on the domain Ω and a positive constant k_2 depending on Γ_0^u, such that

$$\left\|t_\epsilon^\delta - t\right\|_{H_{00}^{\frac{1}{2}}(\Gamma_a)} + \left\|t_\epsilon'^\delta - t'\right\|_{H^{\frac{1}{2}}(\Gamma_0^u)} \leq \frac{\sqrt{2(k_1^2+k_2^2)}}{\epsilon}\|\delta\|_{L^2(\Gamma_0^m)} + h_\epsilon. \tag{6.28}$$

Moreover, if there exist $(y_1, y_2) \in L^2(\Gamma_a)$ and $y_3 \in L^2(\Gamma_0^u)$ such that $t = C^*y_1 + D^*y_2$, $\varphi = B^*y_1$ and $t' = E^*y_2 + F^*y_3$, then the solution satisfies

$$\left\|t_\epsilon^\delta - t\right\|_{H_{00}^{\frac{1}{2}}(\Gamma_a)} + \left\|t_\epsilon'^\delta - t'\right\|_{H^{\frac{1}{2}}(\Gamma_0^u)} \leq \frac{\sqrt{2(k_1^2+k_2^2)}}{\epsilon}\|\delta\|_{L^2(\Gamma_0^m)} + \sqrt{\epsilon}\sqrt{\|y_1\|^2 + \|y_2\|^2 + \|y_3\|^2} \tag{6.29}$$

and

$$\left\|t_\epsilon^\delta - t\right\|^2_{H_{00}^{\frac{1}{2}}(\Gamma_a)} \leq \frac{(k_1^2+k_2^2)}{\epsilon^2}\|\delta\|^2_{L^2(\Gamma_0^m)} + \epsilon\left(\|y_1\|^2 + \|y_2\|^2 + \|y_3\|^2\right) \tag{6.30}$$

Remark 6.2. *The condition $(y_1, y_2) \in L^2(\Gamma_a)$ and $y_3 \in L^2(\Gamma_0^u)$ such that $t = C^*y_1 + D^*y_2$, $\varphi = B^*y_1$ and $t' = E^*y_2 + F^*y_3$ is equivalent to the fact that the triplet solution (φ, t, t') belongs to the image of the operator R^*.*

Proof 6.1. *In order to prove this theorem, we use the following triangle inequality*

$$\begin{aligned}\| t_\epsilon^\delta - t \|_{H_{00}^{\frac{1}{2}}(\Gamma_a)} + \| t_\epsilon'^\delta - t' \|_{H^{\frac{1}{2}}(\Gamma_0^u)} \leq \quad & \| t_\epsilon^\delta - t_\epsilon \|_{H_{00}^{\frac{1}{2}}(\Gamma_a)} + \| t_\epsilon - t \|_{H_{00}^{\frac{1}{2}}(\Gamma_a)} \\ & + \| t_\epsilon'^\delta - t'_\epsilon \|_{H^{\frac{1}{2}}(\Gamma_0^u)} + \| t'_\epsilon - t' \|_{H^{\frac{1}{2}}(\Gamma_0^u)}.\end{aligned}$$

In what follows, we will estimate each of both $\left(\| t'_\epsilon - t' \|_{H_{00}^{\frac{1}{2}}(\Gamma_a)} + \| t_\epsilon - t \|_{H^{\frac{1}{2}}(\Gamma_0^u)}\right)$ and $\left(\| t_\epsilon^\delta - t_\epsilon \|_{H_{00}^{\frac{1}{2}}(\Gamma_a)} + \| t_\epsilon'^\delta - t'_\epsilon \|_{H^{\frac{1}{2}}(\Gamma_0^u)}\right)$ terms separately. For the sake of simplicity and readability we will consider the $\|.\|$ for all the spaces, it refers to $\| \,.\, \|_{H_{00}^{\frac{1}{2}}(\Gamma_a)}$ for $t_\epsilon^\delta, t_\epsilon$ and t, it refers $\| \,.\, \|_{H^{\frac{1}{2}}(\Gamma_0^u)}$ for $t_\epsilon'^\delta, t'_\epsilon$ and t' it refers to $\|.\|_{\left(H_{00}^{\frac{1}{2}}(\Gamma_a)\right)'}$ for $\varphi_\epsilon^\delta, \varphi_\epsilon$ and φ, it refers to $\|.\|_{L^2(\Gamma_0^m)}$ for the noise δ since we only measure on Γ_0^m, and it refers to $\|.\|_{L^2(\theta)}$ for the functions y_1, y_2 and $\|.\|_{L^2(\Gamma_0^u)}$ for y_3.

Estimation of $\| t_\epsilon^\delta - t_\epsilon \|_{H_{00}^{\frac{1}{2}}(\Gamma_a)} + \| t_\epsilon'^\delta - t'_\epsilon \|_{H^{\frac{1}{2}}(\Gamma_0^u)}$

We have

$$\left\langle A_\epsilon \begin{pmatrix} \varphi_\epsilon^\delta - \varphi_\epsilon \\ t_\epsilon^\delta - t_\epsilon \\ t_\epsilon'^\delta - t'_\epsilon \end{pmatrix}, \begin{pmatrix} \varphi_\epsilon^\delta - \varphi_\epsilon \\ t_\epsilon^\delta - t_\epsilon \\ t_\epsilon'^\delta - t'_\epsilon \end{pmatrix} \right\rangle = \left\langle \begin{pmatrix} 0 \\ P\omega(\delta) \\ -\Pi_u \circ P'\delta \end{pmatrix}, \begin{pmatrix} \varphi_\epsilon^\delta - \varphi_\epsilon \\ t_\epsilon^\delta - t_\epsilon \\ t_\epsilon'^\delta - t'_\epsilon \end{pmatrix} \right\rangle,$$

which means

$$\left\langle A \begin{pmatrix} \varphi_\epsilon^\delta - \varphi_\epsilon \\ t_\epsilon^\delta - t_\epsilon \\ t_\epsilon'^\delta - t'_\epsilon \end{pmatrix}, \begin{pmatrix} \varphi_\epsilon^\delta - \varphi_\epsilon \\ t_\epsilon^\delta - t_\epsilon \\ t_\epsilon'^\delta - t'_\epsilon \end{pmatrix} \right\rangle + \epsilon\left\|\varphi_\epsilon^\delta - \varphi_\epsilon\right\|^2 + \epsilon\left\|t_\epsilon^\delta - t_\epsilon\right\|^2 + \epsilon\left\|t_\epsilon'^\delta - t'_\epsilon\right\|^2 =$$

$$\left\langle \frac{1}{\sqrt{\epsilon}} P\omega(\delta), \sqrt{\epsilon}\left(t_\epsilon^\delta - t_\epsilon\right) \right\rangle - \left\langle \frac{1}{\sqrt{\epsilon}} \Pi_u \circ P'\delta, \sqrt{\epsilon}\left(t_\epsilon'^\delta - t'_\epsilon\right) \right\rangle.$$

Since A is symmetric positive, we have

$$\epsilon \left\|t_\epsilon^\delta - t_\epsilon\right\|^2 + \epsilon \left\|t_\epsilon'^\delta - t_\epsilon'\right\|^2 \leq \frac{(k_1^2+k_2^2)}{2\epsilon}\left\|\delta\right\|^2 + \frac{\epsilon}{2}\left[\left\|t_\epsilon^\delta - t_\epsilon\right\|^2 + \left\|t_\epsilon'^\delta - t_\epsilon'\right\|^2\right],$$

where $k_1 = \|Pw\|$ and $k_2 = \|\Pi_u \circ P'\|$. We then obtain

$$\left\|t_\epsilon^\delta - t_\epsilon\right\|^2 + \left\|t_\epsilon'^\delta - t_\epsilon'\right\|^2 \leq \frac{(k_1^2+k_2^2)}{\epsilon^2}\left\|\delta\right\|^2 \tag{6.31}$$

We conclude that

$$\left\|t_\epsilon^\delta - t_\epsilon\right\| + \left\|t_\epsilon'^\delta - t_\epsilon'\right\| \leq \frac{\sqrt{2(k_1^2+k_2^2)}}{\epsilon}\left\|\delta\right\|. \tag{6.32}$$

Estimation of $\left(\| t_\epsilon' - t' \|_{H_{00}^{\frac{1}{2}}(\Gamma_a)} + \| t_\epsilon - t \|_{H^{\frac{1}{2}}(\Gamma_0^u)}\right)$

We have

$$A_\epsilon \begin{pmatrix} \varphi_\epsilon \\ t_\epsilon \\ t_\epsilon' \end{pmatrix} = \begin{pmatrix} 0 \\ P\omega(T_0) \\ -\Pi_u \circ P'T_0 \end{pmatrix} = A \begin{pmatrix} \varphi_\epsilon \\ t_\epsilon \\ t_\epsilon' \end{pmatrix} + \epsilon \begin{pmatrix} \varphi_\epsilon \\ t_\epsilon \\ t_\epsilon' \end{pmatrix} \quad ; \quad A \begin{pmatrix} \varphi \\ t \\ t' \end{pmatrix} = \begin{pmatrix} 0 \\ P\omega(T_0) \\ -\Pi_u \circ P'T_0 \end{pmatrix}.$$

This gives

$$\left\langle A \begin{pmatrix} \varphi_\epsilon - \varphi \\ t_\epsilon - t \\ t_\epsilon' - t' \end{pmatrix}, \begin{pmatrix} \varphi_\epsilon - \varphi \\ t_\epsilon - t \\ t_\epsilon' - t' \end{pmatrix} \right\rangle + \epsilon \left\langle \begin{pmatrix} \varphi_\epsilon \\ t_\epsilon \\ t_\epsilon' \end{pmatrix}, \begin{pmatrix} \varphi_\epsilon - \varphi \\ t_\epsilon - t \\ t_\epsilon' - t' \end{pmatrix} \right\rangle = 0.$$

We then obtain

$$\left\langle A \begin{pmatrix} \varphi_\epsilon - \varphi \\ t_\epsilon - t \\ t_\epsilon' - t' \end{pmatrix}, \begin{pmatrix} \varphi_\epsilon - \varphi \\ t_\epsilon - t \\ t_\epsilon' - t' \end{pmatrix} \right\rangle = -\epsilon \left\langle \varphi_\epsilon, \varphi_\epsilon - \varphi \right\rangle - \epsilon \left\langle t_\epsilon, t_\epsilon - t \right\rangle - \epsilon \left\langle t_\epsilon', t_\epsilon' - t' \right\rangle.$$

On the other side we have

$$\begin{aligned} \langle \varphi_\epsilon, \varphi_\epsilon - \varphi \rangle &= \|\varphi_\epsilon - \varphi\|^2 + \langle \varphi, \varphi_\epsilon - \varphi \rangle \\ \langle t_\epsilon, t_\epsilon - t \rangle &= \|t_\epsilon - t\|^2 + \langle t, t_\epsilon - t \rangle \\ \langle t_\epsilon', t_\epsilon' - t' \rangle &= \|t_\epsilon' - t'\|^2 + \langle t', t_\epsilon' - t' \rangle \end{aligned}$$

Denoting by

$$X_\epsilon = \begin{pmatrix} \varphi_\epsilon - \varphi \\ t_\epsilon - t \\ t_\epsilon' - t' \end{pmatrix},$$

we have

$$\langle AX_\epsilon, X_\epsilon \rangle + \epsilon \|\varphi_\epsilon - \varphi\|^2 + \epsilon \|t_\epsilon - t\|^2 + \epsilon \|t_\epsilon' - t'\|^2 = -\epsilon \langle \varphi, \varphi_\epsilon - \varphi \rangle - \epsilon \langle t, t_\epsilon - t \rangle - \epsilon \langle t', t_\epsilon' - t' \rangle.$$

Using the positivity of A, we have

$$\frac{\epsilon}{2}\left\|\varphi_\epsilon-\varphi\right\|^2+\frac{\epsilon}{2}\left\|t_\epsilon-t\right\|^2+\frac{\epsilon}{2}\left\|t'_\epsilon-t'\right\|^2\leq\frac{\epsilon}{2}\left(\|\varphi\|^2+\|t\|^2+\|t'\|^2\right)$$

Or equivalently

$$\left\|\varphi_\epsilon-\varphi\right\|^2+\left\|t_\epsilon-t\right\|^2+\left\|t'_\epsilon-t'\right\|^2\leq\left(\|\varphi\|^2+\|t\|^2+\|t'\|^2\right)=Cte,$$

where Cte is a positive constant. We then can extract a convergent subsequence

$$\begin{cases}\varphi_\epsilon\longrightarrow\varphi\\ t_\epsilon\longrightarrow t\\ t'_\epsilon\longrightarrow t'\end{cases}\quad \textit{weakly in } H_{00}^{-\frac{1}{2}}\left(\Gamma_a\right)\times H_{00}^{\frac{1}{2}}\left(\Gamma_a\right)\times H_{00}^{\frac{1}{2}}\left(\Gamma_0^u\right).$$

Since,

$$0\leq\lim_{\epsilon\longrightarrow0}\left[\left\|\varphi_\epsilon-\varphi\right\|^2+\left\|t_\epsilon-t\right\|^2+\left\|t'_\epsilon-t'\right\|^2\right]\leq\lim_{\epsilon\longrightarrow0}\left[-\left\langle\varphi,\varphi_\epsilon-\varphi\right\rangle-\left\langle t,t_\epsilon-t\right\rangle-\left\langle t',t'_\epsilon-t'\right\rangle\right]=0,$$

we obtain that

$$\begin{cases}\varphi_\epsilon\longrightarrow\varphi\\ t_\epsilon\longrightarrow t\\ t'_\epsilon\longrightarrow t'\end{cases}\quad \textit{strongly in } H_{00}^{-\frac{1}{2}}\left(\Gamma_a\right)\times H_{00}^{\frac{1}{2}}\left(\Gamma_a\right)\times H_{00}^{\frac{1}{2}}\left(\Gamma_0^u\right).$$

Hence, $\exists h_\epsilon\geq0\underset{\epsilon\longrightarrow0}{\longrightarrow}0$, such that

$$\left\|\varphi_\epsilon-\varphi\right\|+\left\|t_\epsilon-t\right\|+\left\|t'_\epsilon-t'\right\|\leq h_\epsilon \tag{6.33}$$

Combining the inequalities (6.32) *and* (6.33), *we obtain*

$$\left\|t_\epsilon^\delta-t_\epsilon\right\|+\left\|t_\epsilon^{\delta\prime}-t'_\epsilon\right\|+\left\|t_\epsilon-t\right\|+\left\|t'_\epsilon-t'\right\|\leq\frac{\sqrt{2(k_1^2+k_2^2)}}{\epsilon}\|\delta\|+h_\epsilon \tag{6.34}$$

The second estimation

According to the optimality conditions, we do: ((6.23)-(5.20))$\times\left(t_\epsilon-t\right)$ + ((6.24)-(5.21)) $\times\left(\varphi_\epsilon-\varphi\right)$ + ((6.23)-(5.20))$\times\left(t'_\epsilon-t'\right)$ and obtain

$$\begin{aligned}&\epsilon\left\langle t_\epsilon,t_\epsilon-t\right\rangle+\epsilon\left\langle t'_\epsilon,t'_\epsilon-t'\right\rangle+\epsilon\left\langle\varphi_\epsilon,\varphi_\epsilon-\varphi\right\rangle+\left\|D(t_\epsilon-t)+E(t'_\epsilon-t')\right\|^2+\\&+\left\|C(t_\epsilon-t)+B(\varphi_\epsilon-\varphi)\right\|^2+\left\|F(t'_\epsilon-t')\right\|^2=0.\end{aligned} \tag{6.35}$$

We have

$$\epsilon\left\langle t_\epsilon,t_\epsilon-t\right\rangle=\epsilon\left\|t_\epsilon-t\right\|^2+\epsilon\left\langle t,t_\epsilon-t\right\rangle, \tag{6.36}$$

$$\epsilon\left\langle t'_\epsilon,t'_\epsilon-t'\right\rangle=\epsilon\left\|t'_\epsilon-t'\right\|^2+\epsilon\left\langle t',t'_\epsilon-t'\right\rangle, \tag{6.37}$$

$$\epsilon\left\langle\varphi_\epsilon,\varphi_\epsilon-\varphi\right\rangle=\epsilon\left\|\varphi_\epsilon-\varphi\right\|^2+\epsilon\left\langle\varphi,\varphi_\epsilon-\varphi\right\rangle. \tag{6.38}$$

Replacing t by $C^*y_1+D^*y_2$, t' by $E^*y_2+F^*y_3$ and φ by B^*y_1 respectively in the second terms of the right-hand side of equations (6.36), (6.37) *and* (6.38), *respectively. Summing the three equations, we obtain*

$$\begin{aligned}&\epsilon\left\langle t_\epsilon,t_\epsilon-t\right\rangle+\epsilon\left\langle t'_\epsilon,t'_\epsilon-t'\right\rangle+\epsilon\left\langle\varphi_\epsilon,\varphi_\epsilon-\varphi\right\rangle=\epsilon\left\|t_\epsilon-t\right\|^2+\epsilon\left\langle(C^*y_1+D^*y_2),(t_\epsilon-t)\right\rangle\\&+\epsilon\left\|t'_\epsilon-t'\right\|^2+\epsilon\left\langle(E^*y_2+F^*y_3),(t'_\epsilon-t')\right\rangle+\epsilon\left\|\varphi_\epsilon-\varphi\right\|^2+\epsilon\left\langle B^*y_1,\varphi_\epsilon-\varphi\right\rangle.\end{aligned}$$

Regrouping the terms of y_1, y_2 and y_3 and applying the Young inequality we obtain

$$\begin{aligned}
&\epsilon \langle t_\epsilon, t_\epsilon - t\rangle + \epsilon \langle t'_\epsilon, t'_\epsilon - t'\rangle + \epsilon \langle \varphi_\epsilon, \varphi_\epsilon - \varphi\rangle \\
&\geq \epsilon \|t_\epsilon - t\|^2 + \epsilon \|t'_\epsilon - t'\|^2 + \epsilon \|\varphi_\epsilon - \varphi\|^2 - \tfrac{\epsilon^2}{2}\left(\|y_1\|^2 + \|y_2\|^2 + \|y_3\|^2\right) \\
&-\tfrac{1}{2}\left(\|D(t_\epsilon - t) + E(t'_\epsilon - t')\|^2 + \|C(t_\epsilon - t) + B(\varphi_\epsilon - \varphi)\|^2 + \|F(t'_\epsilon - t')\|^2\right).
\end{aligned} \tag{6.39}$$

Injecting this last inequality in the left-hand side of equation (6.35)*, we obtain*

$$\epsilon \|t_\epsilon - t\|^2 + \epsilon \|t'_\epsilon - t'\|^2 + \epsilon \|\varphi_\epsilon - \varphi\|^2 \leq \tfrac{\epsilon^2}{2}\left(\|y_1\|^2 + \|y_2\|^2 + \|y_3\|^2\right). \tag{6.40}$$

Hence, we have

$$\|t_\epsilon - t\| + \|t'_\epsilon - t'\| \leq \sqrt{\epsilon}\sqrt{\left(\|y_1\|^2 + \|y_2\|^2 + \|y_3\|^2\right)}. \tag{6.41}$$

We deduce the second estimation of Theorem 6.1

$$\left\|t^\delta_\epsilon - t\right\| + \left\|t'^\delta_\epsilon - t^{'}\right\| \leq \frac{\|\delta\|}{\epsilon}\sqrt{2(k_1^2 + k_2^2)} + \sqrt{\epsilon}\sqrt{\|y_1\|^2 + \|y_2\|^2 + \|y_3\|^2}.$$

Finally, from (6.31) *and* (6.40)*, we also obtain*

$$\left\|t^\delta_\epsilon - t\right\|^2 \leq \frac{(k_1^2 + k_2^2)}{\epsilon^2}\|\delta\|^2_{L^2(\Gamma_0^m)} + \epsilon\left(\|y_1\|^2 + \|y_2\|^2 + \|y_3\|^2\right). \tag{6.42}$$

6.2. **Complete observation**

In this paragraph, we present an analysis of the Tikhonov regularization [24] in the cylindrical case with total observation of the potential on Γ_0. We will estimate the error between the exact and the regularized problem solution when the observation data T is given on the whole boundary $\Gamma_0^m = \Gamma_0$, and evaluate the effect of noise when considering $(u = T + \delta)$ on Γ_0. We follow the approach developed by Morozov and Stessin [22]. We consider the following problem:

$$(P_0)\begin{cases}
-\Delta u = 0 & \text{in} \quad \Omega, \\
u = 0 & \text{on} \quad \Sigma, \\
\dfrac{\partial u}{\partial n} = 0 & \text{on} \quad \Gamma_0, \\
u = T & \text{on} \quad \Gamma_0, \\
u = t, \ \dfrac{\partial u}{\partial n} = \varphi & \text{on} \quad \Gamma_a.
\end{cases}$$

Using the same definition of u_1 and u_2 as in $(\mathcal{P}_1, \mathcal{P}_2)$, and considering that $\Gamma_0^u = \emptyset$, the cost functional with total observation is:

$$\begin{aligned}
J(\eta,\tau) &= \int_\Omega |\nabla u_1 - \nabla u_2|^2\, dxdy. \\
J(\eta,\tau) &= Cte + (\eta,\tau)\, A\begin{pmatrix}\eta \\ \tau\end{pmatrix} - 2\langle \omega(T), P\tau\rangle.
\end{aligned}$$

$$\inf_{\eta,\tau} J(\eta,\tau) = J(\varphi, t) = 0.$$

where the operators matrix is defined by:

$$A = \begin{pmatrix} Q & -QP \\ -PQ & P \end{pmatrix}.$$

For non negative values of ϵ, the cost functional with the Tikhonov regularization is defined as follows

$$J_\epsilon(\eta,\tau) = Cte + (\eta,\tau)\, A \begin{pmatrix} \eta \\ \tau \end{pmatrix} - 2\,\langle \omega(T), P\tau\rangle + \epsilon \left(\|\eta\|^2_{\left(H^{\frac{1}{2}}_{00}(\Gamma_a)\right)'} + \|\tau\|^2_{H^{\frac{1}{2}}_{00}(\Gamma_a)} \right),$$

We also define a cost function for the noisy data and Tikhonov regularization as follows

$$J^\delta_\epsilon(\eta,\tau) = Cte + (\eta,\tau)\, A \begin{pmatrix} \eta \\ \tau \end{pmatrix} - 2\,\langle \omega(T+\delta), P\tau\rangle + \epsilon \left(\|\eta\|^2_{\left(H^{\frac{1}{2}}_{00}(\Gamma_a)\right)'} + \|\tau\|^2_{H^{\frac{1}{2}}_{00}(\Gamma_a)} \right).$$

The aim of the following theorem is to give an estimate of the reconstructed electrical potential when considering noisy data on the complete accessible boundary. Following the same strategy used in the incomplete boundary case, we apply a Cholesky factorization of the operator A.

$$A = R^* R \quad \text{where} \quad R = \begin{pmatrix} B & C \\ 0 & D \end{pmatrix}$$

By identification, we have

$$\begin{cases} B = Q^{\frac{1}{2}}, \\ C = -Q^{\frac{1}{2}} P, \\ D = (P - PQP)^{\frac{1}{2}}, \end{cases}$$

One could check that operators P, Q and $I - P\,Q$ are positive.

Theorem 6.3. *Let's denote by (φ, t), the exact solution and $\left(\varphi^{\delta,c}_\epsilon, t^{\delta,c}_\epsilon\right)$ the solution of the regularized problem with noisy data. Then, we have*

$$\left\|t^{\delta,c}_\epsilon - t\right\|_{H^{\frac{1}{2}}_{00}(\Gamma_a)} \le \frac{k_1}{\epsilon} \|\delta\|_{L^2(\Gamma_0)} + g_\epsilon \tag{6.43}$$

where

$$g_\epsilon \ge 0 \text{ and } g_\epsilon \longrightarrow 0 \text{ for } \epsilon \longrightarrow 0$$

Moreover, if $(\varphi, t) \in Im(R^*)$ meaning that there exist $y_1, y_2 \in L^2(\Gamma_a)$ such that $\varphi = B^* y_1$ and $t = C^* y_1 + D^* y_2$, then we have

$$\left\|t^{\delta,c}_\epsilon - t\right\|^2_{H^{\frac{1}{2}}_{00}(\Gamma_a)} \le \frac{k_1^2}{\epsilon^2} \|\delta\|^2_{L^2(\Gamma_0)} + \epsilon \left(\|y_1\|^2 + \|y_2\|^2 \right) \tag{6.44}$$

The proof of Theorem 6.3, uses exactly the same arguments developed in the proof of Theorem6.1. The second condition in the theorem is satisfied when the Cauchy data is sufficiently regular as shown in the following lemma.

Lemma 6.4. *For a given electrical potential T compatible with zero flux boundary condition, if (t, φ) is solution of the data completion problem, then we can find y_1 and y_2 such as $y_1 \in L^2(\theta)$, $y_2 \in L^2(\theta)$ such as $\varphi = B^* y_1$ and $t = C^* y_1 + D^* y_2$, as soon as $T \in H^{\frac{3}{2}}(\theta)$.*

The proof of the Lemma 6.4 is given in the appendix and it uses the modal decomposition of the Laplace operator on the transverse direction.

6.3. Theoretical interpretation of the measurement boundary size and the distribution of noise effects on the reconstructed solution

In terms of convergence rate, the theoretical estimations shown in the Theorem 6.3 and Theorem 6.1 provide the same rate of convergence in terms of the noise δ and in terms of the regularization parameter ϵ. The difference between complete and incomplete measurement cases is in the constants of the convergence. This could reflect if the one or the other is much more appropriate depending on the distribution of the noise. Let's denote by E^c the maximal error on the electrical potential on the heart boundary Γ_a in the case where we measure on the whole accessible Γ_0.

$$\begin{aligned} E^c(\epsilon,\delta): &= \tfrac{k_1^2}{\epsilon^2}\|\delta\|^2_{L^2(\Gamma_0)} + \epsilon\left(\|y_1\|^2 + \|y_2\|^2\right) \\ &= \tfrac{k_1^2}{\epsilon^2}\left(\|\delta\|^2_{L^2(\Gamma_0^m)} + \|\delta\|^2_{L^2(\Gamma_0^u)}\right) + \epsilon\left(\|y_1\|^2 + \|y_2\|^2\right). \end{aligned}$$

On the other side, we denote by E^i the maximal error in the case where we measure only on the subboundary Γ_0^m

$$E^i(\Gamma_0^m,\epsilon,\delta) := \frac{(k_1^2 + k_2^2)}{\epsilon^2}\|\delta\|^2_{L^2(\Gamma_0^m)} + \epsilon\left(\|y_1\|^2 + \|y_2\|^2 + \|y_3\|^2\right).$$

The difference between both error bounds reads

$$E^c(\epsilon,\delta) - E^i(\Gamma_0^m,\epsilon,\delta) = \frac{k_1^2}{\epsilon^2}\|\delta\|^2_{L^2(\Gamma_0^u)} - \frac{k_2^2}{\epsilon^2}\|\delta\|^2_{L^2(\Gamma_0^m)} - \epsilon\|y_3\|^2.$$

From this we distinguish two cases depending on the distribution of the noise δ:

- If $\|\delta\|^2_{L^2(\Gamma_0^u)} < \dfrac{k_2^2}{k_1^2}\|\delta\|^2_{L^2(\Gamma_0^m)} + \dfrac{\epsilon^3}{k_1^2}\|y_3\|$, then it is worth to use all the available measurement at Γ_0.
- If $\|\delta\|^2_{L^2(\Gamma_0^u)} > \dfrac{k_2^2}{k_1^2}\|\delta\|^2_{L^2(\Gamma_0^m)} + \dfrac{\epsilon^3}{k_1^2}\|y_3\|$, then it is worth to only use the measurements on Γ_0^m

Remark 6.5. *In practice $\|y_3\|$ is not available, but since this term is multiplied by ϵ^3, the term $\frac{\epsilon^3}{k_1^2}\|y_3\|$ might be neglected. This problem could be avoided using simulated data for which one has exact solution and thus could construct y_1, y_2, y_3. Then one could test if the distribution of noise is much more suitable for full observation on Γ_0 or incomplete mesaurements on Γ_0^m using simulated data.*

Remark 6.6. *When interpolation is performed like in [11, 13, 23] it is important to build an estimator of the interpolation error, which could then be used to decide whether or not to use the interpolated data.*

Remark 6.7. *The error bounds here do not take into account the errors related to the discretization of the problem. It would be interesting to add the discretization error to the comparison result.*

7. Numerical method

In this section, we present the results of numerical simulations to solve the data completion problem (p_0) on a rectangular area using the invariant embedding technique developed in the previous sections. The idea is to test the effect and the area that lacks data method for a problem where an analytical solution is known. Thus it is possible to accurately compare results that are "reconstructed" and "analytical".
We consider problem (p_0) on $]0,a[\times]0,2\pi[$. x is the variable which describes the area of length between 0 and a, while y is the one which crosses the transverse coordinate between 0 and π. The Cauchy data on Γ_0 are $u(x,y)_{|\Gamma_0^m} = u(0,y)_{|\Gamma_0^m} = T = \sin(y)$ and $\dfrac{\partial u}{\partial n}u(x,y)_{|\Gamma_0} = \dfrac{\partial u}{\partial n}(0,y)_{|\Gamma_0} = 0$ and is seeking to rebuild the data on the surface Γ_a. One could check that the harmonic function $u(x,y) = \cosh(x)\sin(y)$ is the solution of the problem. The data to be completed on Γ_a are: $t_{\text{theo}} = u(a,y) = \cosh(a)\sin(y)$ and

$\varphi_{\text{ theo}} = \dfrac{\partial u}{\partial n}(a, y) = \sinh(a)\sin(y)$ and on Γ_0^u we also construct $t'_{\text{theo}} = u(0, y) = \sin(y)$. We use a finite difference method for the numerical solution of (4.5) and (4.7). To do this we denote by n the number of points along the length x-direction and p the number of points along the transverse direction y. We define by $u(ih, jk)$ the solution of the problem at the grid points coordinates $x = ih$, $y = jk$. This discretization is done in two separate steps. The first follows the transverse direction and that turns the discrete Dirichlet-Neumann and Neumann-Dirichlet operators in matrices respectively P_i and Q_i at $x = ih$, $0 \leq i \leq n$. These matrices are then of size $(p-1) \times (p-1)$ that connects the values u_i of the solution at the grid points on section $x = ih$ to the approximation of derivative on the same section. These matrices satisfy Riccati equations along the x variable. The second step consists in the discretization along the axis of dipping, that is to say in x. It then applies a Euler scheme operators to resolve and determine on the surface $x = a$ is the same procedure for solving the residuals. The first discretization defines the matrix of size $\omega\ (p-1) \times 1$ and also checking the equations residue. The second allows, also using an Euler scheme to determine the ω on the surface for missing data. Finally, we must build the interface operator and solve linear problems to determine t_{num} and t'_{num}. After a discretization in the x direction, this equation is solved by an explicit Euler scheme respecting stability conditions.

$$\begin{cases} P_i = P_{i-1}\left(I - hP_{i-1}\right) - h\Delta_{T,k}, \\ P(0)_{|\Gamma_0} = 0. \end{cases}$$

where $\Delta_{T,k}$ is the three diagonal matrix associated with the three points approximation to the second derivative. A similar scheme is applied to the Neumann-Dirichlet operator

$$\begin{cases} Q_i = Q_{i-1}\left(I - h\Delta_{T,k}Q_{i-1}\right) - hI, \\ Q(0)_{|\Gamma_0^m} = 0, \quad Q(0)_{|\Gamma_0^u} = 0. \end{cases}$$

and to the residual equation :

$$\begin{cases} \omega_i = \left(I - h\Delta_{T,k}Q_{i-1}\right)\omega_{i-1} \\ \omega(0)_{|\Gamma_0^m} = 0, \quad \omega(0)_{|\Gamma_0^u} = 0 \end{cases},$$

The equations of operators S P' and H are solved similarly. The scheme has been implemented in MATLAB. In order to be able to compare the results with different level of noise, we generated a normalized white noise using the rand function of matlab. This noise is saved and is used for all test cases, it will be just fully or partially rescaled in order to produce different levels of noise. In the following simulations we took $p = 201$, $n = 2000$, $a = \pi$ $b = 2\pi$ and $\epsilon = 10^{-6}$. We shall also say that in what follows the measurement boundary is placed in the center of Γ_0. For a given percentage α, we define Γ_0^m as the interval $[\frac{b}{2}(1 - \frac{\alpha}{100}), \frac{b}{2}(1 + \frac{\alpha}{100})]$

8. Results

In this section we will conduct to two test cases reflecting the theoretical results that we obtained. In the first test case we will use a homogeneous white noise, which means that the level of noise is the same in all the boundary Γ_0. This does not mean that the noise is constant, it only means that point-wise, the absolute value of the noise is less than a given constant. In this case, we are mimicking the fact that the electrodes cover the whole accessible domain Γ_0 and that the electrodes have the same measurement error. We will look how loosing part of these electrodes measurements affects the reconstructed solution.

In the second case, we consider that either part of electrodes are missing or that it is measuring but with a high level of noise. In the case that part of the electrodes is missing we suppose that one could use an interpolation method and depending on the error of interpolation we will look if considering these interpolated signals improves or deteriorates the solution.

8.1. **Homogeneous noise**

In this paragraph, we test the effect of size of the sub-boundary of measurements Γ_0^m and the different levels of noise on the quality of the reconstructed solution on the inaccessible boundary Γ_a. We vary the size of Γ_0^m from 20% to 100% of the full accessible boundary. We also vary the level of noise from 0% to 30%. In figure 4 (respectively, figure 4), we measure T on 50% (respectively, 90%) of Γ_0, the measurements contain 10% (respectively, 20%) of noise as shonw in the left panel. The obtained solution on the "heart" boundary Γ_a is shown in the left panel (red continuous line) where we compare it to the exact solution (blue dashed line). The relative error with respect to the exact solution is 0.26 (respectively, 0.18).

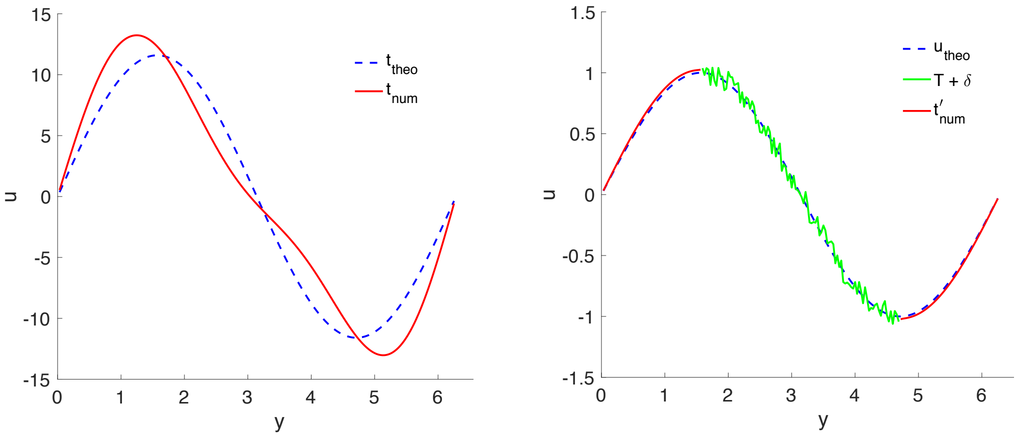

FIGURE 3. Left: Comparison between the exact solution (blue dashed ligne) and the incomplete boundary measurement inverse solution (red continuous line). Right solutions with respect to the noise level at Γ_0^u. The noise on the measured boundary Γ_0^m does not not change Γ_0^m occupies 50% of Γ_0 and the noise level is 10% . Right: Reconstructed solution on the accessible unmeasured boundary Γ_0^u (red continuous line), Noisy measurement $T + \delta$ (green continuous line) and exact solution on Γ_0 (blue dashed line).

In Table 8.1, we present the relative error of the reconstructed potential t_{num}on Γ_a with respect to the theoretical solution. Looking at each raw of the Table 8.1, we remark that the relative error increases monotonously when increasing the level of noise and this is independent of size of the measurement domain Γ_0^m. On the other side, looking at the columns of Table 8.1, we remark that the error does not decrease monotonously when increasing the size of the measurement boundary Γ_0^m for each level of noise. Although, it is the case for low level of noise (0%, 1%, 5%, 10 %), for high level of noise (20%, 30%), we see the error increases when the size of Γ_0^m increases from 20% to 30%, and then decreases monotonously. We think that the distribution of the noise is the main reason.

8.2. **Non homogeneous noise**

Here we suppose that either some electrodes are defective or certain regions of the accessible boundary are not covered by electrodes. We also suppose that the user want to make some interpolation on this region. We assume here that the error of interpolation would be combined to the error of measurement leading to a new noise level on the boundary Γ_0^u different from the noise on Γ_0^m. In what follows we don't do any interpolation we progressively increase the level of noise on the unmeasured boundary Γ_0^u and we compare the solutions of the following two cases: In the first case, we only use the measurements recorded by the non defective electrodes on Γ_0^m and solve the inverse problem with an incomplete information on the accessible boundary we denote the relative error E^i as previously denoted in the analysis section. In the second case we use the

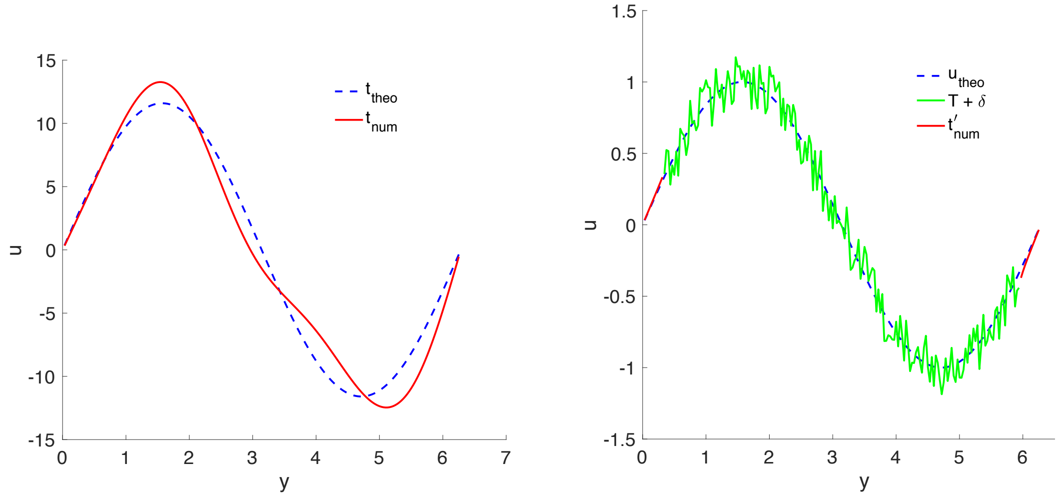

FIGURE 4. Left: Comparison between the exact solution (blue dashed ligne) and the incomplete boundary measurement inverse solution (red continuous line). Right solutions with respect to the noise level at Γ_0^u. The noise on the measured boundary Γ_0^m does not not change Γ_0^m occupies 50% of Γ_0 and the noise level is 10% . Right: Reconstructed solution on the accessible unmeasured boundary Γ_0^u (red continuous line), Noisy measurement $T + \delta$ (green continuous line) and exact solution on Γ_0 (blue dashed line).

Γ_0^m% \ noise %	0%	1%	5%	10%	20%	30%
20%	0.6151	0.6169	0.6261	0.6417	0.6847	0.7414
30%	0.4358	0.4491	0.5078	0.5901	0.7723	0.9666
50%	0.0894	0.1067	0.1769	0.2655	0.4433	0.6213
60%	0.0312	0.0394	0.1076	0.2036	0.3989	0.5949
80%	0.0062	0.0166	0.0710	0.1399	0.2780	0.4160
90%	0.0059	0.0116	0.0480	0.0950	0.1891	0.2833
100%	0.0059	0.0084	0.0275	0.0532	0.1052	0.1572

TABLE 1. Relative error between the exact solution and the solution obtained using different measurement subboundaries (raws) and different level of noise (columns), $(a = \pi, b = 2\pi)$.

noisy data in all the accessible boundary Γ_0 and we denote by E^c the corresponding relative error. In Figure 5 (left, respectively right) the measurement boundary Γ_0^m occupies 80% (respectively, 50%) of Γ_0. Using a noise level of 2% (respectively, 5%), the relative error E^i is 0.03 (respectively, 0.17) see blue constant line in both panels. We remark that for a noise level less than 14% (respectively 30%) on Γ_0^u, while keeping the noise level 2% (respectively 5%) on Γ_0^m, the relative error of the complete measurements case solution is better than incomplete case solution, the red line is under the blue line. While for higher level of noise on Γ_0^m, the complete measurement case solution becomes worst than the incomplete one. This reflects the theoretical result that we obtained in the section of comparison between E^i and E^c.

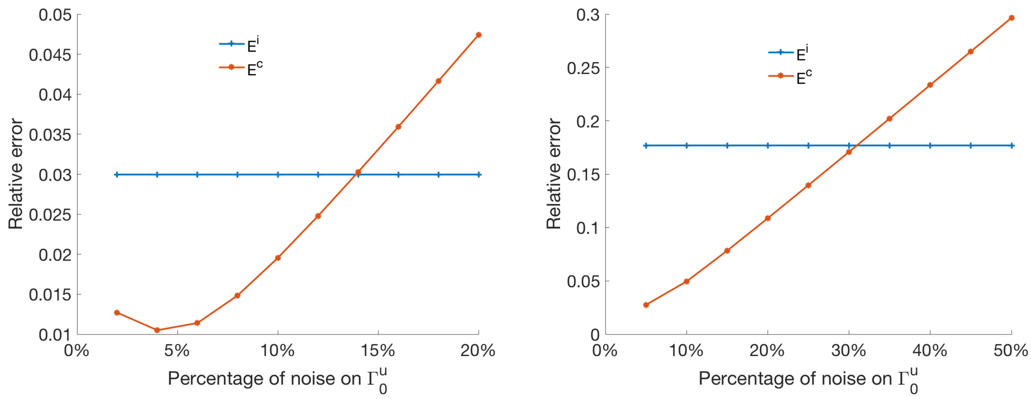

FIGURE 5. Comparison between the incomplete boundary measurment (blue ligne) and the complete boundary measurement (red line) inverse solutions with respect to the noise level at Γ_0^u. The noise on the measured boundary Γ_0^m does not not change. Left figure Γ_0^m occupies 80% and the fixed noise is 2%. Right figure Γ_0^m occupies 50% and the fixed noise is 5%.

8.3. **An Oscillating case**

In order to show how the method performs in an oscillating case, we change here the analytical expression of the solution by adding another frequency in the y-direction. The new function we look for is

$$u(x,y) = \sin(y)\cosh(x) + 4\sin(\frac{y}{2})\cosh(\frac{x}{2})$$

the space domain is $[0, 1.5\pi] \times [0, 8\pi]$. The measured boundary is $\Gamma_0^m = 0 \times [0.8\pi, 7.2\pi]$ which corresponds to 80% of Γ_0 and the noise percentage $\delta = 20\%$ see Figure 6 (right) . The relative error of the solution shown in Figure 6 (left) is 13%.

CONCLUSION

In this paper, we presented a method to solve a data completion problem for the electrocardiography imaging inverse problem. The Cauchy data are measured on the part of the accessible boundary. In our case the Neumann boundary condition is given in the whole accessible domain. We used a method based on the factorization of elliptic boundary value problems. We analyzed the error in case of measurements on all the accessible domain and when only part of the accessible domain is measured. We obtained a comparison result between both cases depending on the distribution of the noise on Γ_0 We numerically tested this method on a 2D rectangular domain. We obtained the following results: 1) for a fixed Γ_0^m, the error increases monotonously with the level of noise and this is independent of size of the measurement domain Γ_0^m; 2) for a fixed noise level, there is no guarantee that error decreases while increasing the size of the measurement boundary Γ_0^m. Our conclusion is that depends on how the noise is distributed in Γ_0. 3) by progressively increasing the noise level on Γ_0^u while the noise level is fixed on Γ_0^m, one could numerically find the critical noise level on Γ_0^u from which there is no gain in considering the data Γ_0^u. This result could be practically used if one has an estimator of the interpolation error in the unmeasured boundary. The numerical analysis of this problem taking into account 3D realistic data both in the geometry and the measurements, taking into account the noise in the measured boundary but also the numerical errors in the computation of all the operators would be subject of a forthcoming work.

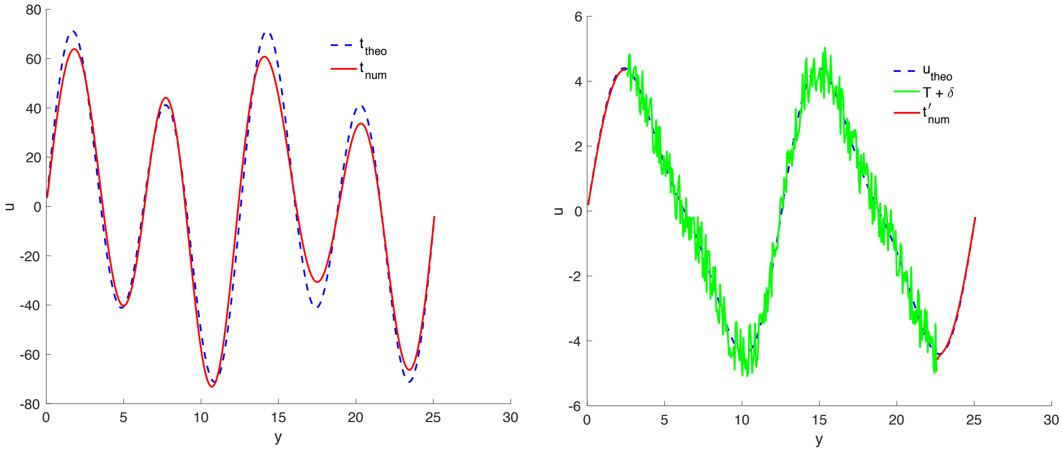

FIGURE 6. Comparison between the exact solution (blue dashed ligne) and the incomplete boundary measurement inverse solution (red continuous line). Right solutions with respect to the noise level at Γ_0^u. The noise on the measured boundary Γ_0^m does not not change Γ_0^m occupies 80% of Γ_0 and the noise level is 20% (left). Reconstructed solution on the accessible unmeasured boundary Γ_0^u (red continuous line), Noisy measurement $T + \delta$ (green continuous line) and exact solution on Γ_0 (blue dashed line) (right).

ACKNOWLEDGEMENTS.

This work has been supported by EPICARD cooperative research program, funded by INRIA international laboratory LIRIMA. The LAMSIN researcher's work is supported on a regular basis by the Tunisian Ministry of Higher Education, Scientific Research and Technology. This study received also financial support from the French Government as part of the 'Investments of the future' program managed by the National Research Agency (ANR), Grant reference ANR-10-IAHU-04.

9. APPENDIX: PROOF OF LEMMA 6.4

Proof 9.1. *Since we look for y_1 and y_2 in $L^2(\theta)$ such that $\varphi = B^* y_1$ and $t = C^* y_1 + D^* y_2$, we formally have $\varphi = Q^{\frac{1}{2}} y_1$. This means that*

$$y_1 = Q^{-\frac{1}{2}} \varphi.$$

On the other side, we have $\varphi = Pt$, this means that $t = P^{-1}\varphi$

$$t = P^{-1}\varphi = D^* y_2 - C^* y_1 = D^* y_2 - P\varphi.$$

This means that $D^* y_2 = (P^{-1} + P)\varphi$.
We begin by proving that we can find y_2 such that $D^* y_2 = \left(P^{-1} + P\right)\varphi$. We decompose the Dirichlet data T on the basis of eigenfunctions $(e_i)_{i>0}$ of Δ_θ the Laplacian on the transverse direction θ;

$$T = \sum_i T_i e_i.$$

Then we have

$$t = \sum_i T_i \exp\left(- \int_0^a \lambda_i \tanh(\lambda_i x)\, dx \right) e_i$$

and since $\varphi = Pt$, *we have*

$$\varphi = \sum_i \lambda_i T_i \tanh(\lambda_i a) \exp\left(-\int_0^a \lambda_i \tanh(\lambda_i x)\,dx\right) e_i$$

we multiply by $\left(P^{-1}+P\right)$:

$$\left(P^{-1}+P\right)\varphi = \sum_i \left(\lambda_i^2 \tanh^2(\lambda_i a)+1\right) T_i \exp\left(-\int_0^a \lambda_i \tanh(\lambda_i x)\,dx\right) e_i$$

we remark that

$$\exp\left(-\int_0^a \lambda_i \tanh(\lambda_i x)\,dx\right) = \frac{1}{\cosh(\lambda_i a)}.$$

On the orther side, we have $D = (P - PQP)^{\frac{1}{2}}$, *its eigenvalues are*

$$(\lambda_i \tanh(\lambda_i a))^{\frac{1}{2}} \frac{1}{\cosh(\lambda_i a)}.$$

Thus we can define y_2 *by*

$$\begin{aligned} y_2 &= \sum_i \frac{\left(\lambda_i^2 \tanh^2(\lambda_i a)+1\right)}{\cosh(\lambda_i a)} . \frac{\cosh(\lambda_i a)}{(\lambda_i \tanh(\lambda_i a))^{\frac{1}{2}}} T_i e_i \\ &= \sum_i \frac{1}{(\lambda_i \tanh(\lambda_i a))^{\frac{1}{2}}} + (\lambda_i \tanh(\lambda_i a))^{\frac{3}{2}} T_i e_i. \end{aligned}$$

Hence, y_2 *is well defined in* $L^2(\theta)$ $\left(\sum\limits_i \left(y_2^i\right)^2 < +\infty\right)$ *as soon as* $\sum\limits_i \lambda_i^3 T_i^2 < +\infty$, *which is equivalent to the fact that* $T \in H^{\frac{3}{2}}(\theta)$.
Using the same strategy, we can find y_1 *defined as follows*

$$\begin{aligned} y_1 &= Q^{-\frac{1}{2}}\varphi \\ &= \sum_i \frac{(\lambda_i)^{\frac{1}{2}}}{(\tanh(\lambda_i a))^{\frac{1}{2}}} \lambda_i \frac{\tanh(\lambda_i a)}{\cosh(\lambda_i a)} T_i e_i \\ &= \sum_i (\lambda_i)^{\frac{3}{2}} \frac{(\tanh(\lambda_i a))^{\frac{1}{2}}}{\cosh(\lambda_i a)} T_i' e_i. \end{aligned}$$

We have $y_1 \in L^2$ $\left(\sum\limits_i \left(y_1^i\right)^2 < +\infty\right)$ *for* $T \in H^{\frac{3}{2}}(\theta)$.

References

[1] Amel Ben Abda, Jacques Henry, and Fadhel Jday. Boundary data completion: the method of boundary value problem factorization. *Inverse Problems*, 27(5):055014, 2011.

[2] Rajae Aboulaich, Amel Ben Abda, and Moez Kallel. Missing boundary data reconstruction via an approximate optimal control. *Inverse Problems & Imaging*, 2(4):411–426, 2008.

[3] Rajae Aboulaich, Amel Ben Abda, and Moez Kallel. A control type method for solving the cauchy–stokes problem. *Applied mathematical modelling*, 37(6):4295–4304, 2013.

[4] Rajae Aboulaich, Najib Fikal, E El Guarmah, and N Zemzemi. Stochastic finite element method for torso conductivity uncertainties quantification in electrocardiography inverse problem. *Mathematical Modelling of Natural Phenomena*, 11(2):1–19, 2016.

[5] Stephane Andrieux, Amel Ben Abda, and Thouraya Nouri Baranger. Data completion via an energy error functional. *Comptes Rendus Mécanique*, 333(2):171–177, 2005.

[6] Mejdi Azaïez, Faker Ben Belgacem, and Henda El Fekih. On cauchy's problem: Ii. completion, regularization and approximation. *Inverse problems*, 22(4):1307, 2006.

[7] Roger C Barr, Maynard Ramsey III, and Madison S Spach. Relating epicardial to body surface potential distributions by means of transfer coefficients based on geometry measurements. *Biomedical Engineering, IEEE Transactions on*, pages 1–11, 1977.

[8] Laura Bear, Mark Potse, Josselin Duchateau, Nejib Zemzemi, Yves Coudière, and Rémi Dubois. Accuracy of lead removal vs linear interpolation in non-invasive electrocardiographic imaging (ecgi). In *Computing in Cardiology Conference (CinC), 2015*. IEEE, 2014.

[9] Richard Ernest Bellman and Howard A Osborn. *Dynamic programming and the variation of Green's functions.* RAND Corporation, 1957.

[10] Julien Bouyssier, Nejib Zemzemi, and Jacques Henry. Inverse problem in electrocardiography via factorization method of boundary problems: how reconstruct epicardial potential maps from measurements of the torso? In *International Symposium on Biomedical Imaging (ISBI), 2015*. IEEE, 2015.

[11] John E Burnes, David C Kaelber, Bruno Taccardi, Robert L Lux, Philip R Ershler, and Yoram Rudy. A field-compatible method for interpolating biopotentials. *Annals of biomedical engineering*, 26(1):37–47, 1998.

[12] A Chakib and A Nachaoui. Convergence analysis for finite element approximation to an inverse cauchy problem. *Inverse Problems*, 22(4):1191, 2006.

[13] Alireza Ghodrati, Dana H Brooks, and Robert S MacLeod. Methods of solving reduced lead systems for inverse electrocardiography. *Biomedical Engineering, IEEE Transactions on*, 54(2):339–343, 2007.

[14] Jacques Hadamard. *Lectures on Cauchy's problem in linear partial differential equations.* Courier Corporation, 2014.

[15] Nejla Hariga-Tlatli, TN Baranger, and Jocelyne Erhel. Misfit functional for recovering data in 2d electrocardiography problems. *Engineering Analysis with Boundary Elements*, 34(5):492–500, 2010.

[16] Jacques Henry and AM Ramos. Factorization of second-order elliptic boundary value problems by dynamic programming. *Nonlinear Analysis: Theory, Methods & Applications*, 59(5):629–647, 2004.

[17] Jacques Henry and Angel M Ramos. Study of the initial value problems appearing in a method of factorization of second-order elliptic boundary value problems. *Nonlinear Analysis: Theory, Methods & Applications*, 68(10):2984–3008, 2008.

[18] Jacques Henry and Angel M Ramos. *La méthode de factorisation des problèmes aux limites par plongement invariant.* ISTE editions, 2016.

[19] Fadhel Jday. *Complétion de données frontieres: la méthode de plongement invariant.* PhD thesis, PHD thesis, 2012.

[20] Vladimir Arkad'evich Kozlov, Vladimir Gilelevich Maz'ya, and AV Fomin. An iterative method for solving the cauchy problem for elliptic equations. *Zhurnal Vychislitel'noi Matematiki i Matematicheskoi Fiziki*, 31(1):64–74, 1991.

[21] Jacques Louis Lions and Enrico Magenes. *Problemes aux limites non homogenes et applications.* Dunod, 1968.

[22] Vladimir Alekseevich Morozov and Michael Stessin. *Regularization methods for ill-posed problems.* CRC press Boca Raton, FL:, 1993.

[23] Thom F Oostendorp, Adriaan van Oosterom, and Geertjan Huiskamp. Interpolation on a triangulated 3d surface. *Journal of Computational Physics*, 80(2):331–343, 1989.

[24] A.N. Tikhonov and V. Arsenin. Solutions of ill-posed problems. *WH Winston, Washington, DC*, 1977.

[25] Yong Wang and Yoram Rudy. Application of the method of fundamental solutions to potential-based inverse electrocardiography. *Annals of biomedical engineering*, 34(8):1272–1288, 2006.

[26] Nejib Zemzemi. A steklov-poincaré variational formulation of the inverse problem in cardiac electrophysiology. In *CinC-Computing in Cardiology Conference*, page 193. IEEE, 2013.

[27] Nejib Zemzemi, Hamed Bourenane, and Hubert Cochet. An iterative method for solving the inverse problem in electrocardiography imaging: From body surface to heart potential. In *Computing in Cardiology Conference (CinC), 2014*, pages 717–720. IEEE, 2014.